UNIVERSITY OF HELSINKI
FACULTY OF BIOLOGICAL AND ENVIRONMENTAL SCIENCES

Master's thesis

Master's Programme in Ecology and Evolutionary Biology

Dynamic tRNA and rRNA modificome changes upon oxidative stress

Student:

Silvija Milosavljević

Supervisors:

Peter Sarin, PhD, Docent in Molecular Biology

Ulrike Abendroth, PhD, Postdoctoral Researcher

RNAcious Laboratory

HELSINGIN YLIOPISTO
HELSINGFORS UNIVERSITET
UNIVERSITY OF HELSINKI

Tiedekunta – Fakultet – Faculty **Faculty of Biological and Environmental Sciences**		Koulutusohjelma – Utbildningsprogram – Degree Programme **Master's Programme in Ecology and Evolutionary Biology**
Tekijä – Författare – Author **Silvija Milosavljević**		
Työn nimi – Arbetets titel – Title **Dynamic tRNA and rRNA modificome changes upon oxidative stress**		
Oppiaine/Opintosuunta – Läroämne/Studieinriktning – Subject/Study track **Ecology and Evolutionary Biology**		
Työn laji – Arbetets art – Level **MSc**	Aika – Datum – Month and year **May 2021**	Sivumäärä – Sidoantal – Number of pages **70**

Tiivistelmä – Referat – Abstract

Post-transcriptional modifications (PTMs) in RNA are present in all known RNA species and conserved in all kingdoms of life. Transfer RNA (tRNA) has been shown to have numerous conserved modifications, which exemplifies the importance of modifications having impact on the structure of the tRNA and its function as carrier of the amino acids. Ribosomal RNAs (rRNA) are universally modified as well, and modifications are situated at functionally important spots of the ribosome. Given the fact that types and sites of modifications are conserved, it is likely that these modifications have been selected for and that they optimize the ribosomal structure and functions.

Stress, such as temperature or infection by a pathogen, is known to change the presence or abundance of modifications in RNA molecules and thereby affect translation efficacy. In line with that, this master's thesis project sought to gain insight into the dynamics of PTMs in tRNA and rRNA upon oxidative stress, with the goal of utilizing recently optimized UPLC/MS method for identifying modified ribonucleosides. As the specific aim of the thesis was to estimate the change in PTMs in tRNA and rRNA in response to oxidative stress with 0.5 mM and 2 mM hydrogen peroxide H_2O_2, 3 immediate goals were: (i) to isolate total tRNA from yeast grown in stress conditions, (ii) to isolate rRNA from yeast 80S ribosomes, and (iii) to identify present modifications using mass spectrometry.

Yeast was cultured in presence of H_2O_2 as a stressor in mentioned concentrations, and both treatments considered showed a difference in survival when compared to the control. Rough cell concentration estimates (OD_{600}) did not show the effect of the stressor on cell survival clearly, but when number of viable cells per mL was estimated, it was clear that growth of the stressed yeast cultures was hindered 2 hours after exposure to H_2O_2 but recovered during the 24 hours.

Firstly, using UPLC/MS analysis, 29 modifications were identified in tRNA from control and H_2O_2 treated yeast. Most identified modifications showed no change in abundance in treatments, which is to be verified with additional replicates. However, distinct dynamics of stress-related change was found for several modifications, revealing additional modifications that may play a role in stress related modificome reprogramming to the previously known signature modifications of oxidative stress.

It was expected that recovery of culture growth after 24 hours may be accompanied with modification level recovery. However, that was not demonstrated here as downregulation at 2 hours followed by upregulation at 24 hours was seen for 2-methylthio-*N6*-methyladenosine, *N4*-acetylcytidine and 5-methoxycarbonylmethyl-2-thiouridine, and the reverse was shown for *N4*-methylcytidine. Upregulation in both time points was also shown here for some modifications. Taken together, these results confirm a complex and dynamic control of tRNA modifications in cellular survival responses.

Modifications found to be affected by oxidative stress are most frequently located on the wobble position 34 and anticodon loop position 37, so it is expected that changes in their modification levels could directly affect the tRNA function in translation, making them a specific target for future research.

Secondly, modifications in rRNA from control yeast cultures were identified, such as expected methylations of all 4 canonical nucleosides. However, further analysis will be needed to confirm the other identified modifications, due to the potential mRNA and tRNA contamination. Optimizing the method for rRNA modifications identifications by acquiring more modified nucleosides specific for the rRNA to use as standards in the analysis, analyzing rRNA types separately and using tandem mass spectrometry would enable getting a deeper understanding of which modifications are present and where they are positioned. Finally, it would enable reliable identification of the signals of novel modifications present in rRNA, such as the tRNA modification 5-carbamoylmethyluridine signal found here.

In conclusion, this thesis work lays the foundation to study the evolutionary conserved function of PTM changes during stress as modulators of translation, using the methodological approaches discussed in-depth within the thesis, primarily to confirm the intriguing results found here.

Avainsanat – Nyckelord – Keywords
Transfer RNA, Ribosomal RNA, Post-transcriptional modifications, Yeast, Oxidative stress

Ohjaaja tai ohjaajat – Handledare – Supervisor or supervisors
Peter Sarin, PhD
Ulrike Abendroth, PhD (co-supervisor)

Säilytyspaikka – Förvaringsställe – Where deposited
HELDA - Helsingin yliopiston digitaalinen arkisto / HELDA - Helsingfors universitets digitala publikationsarkiv / HELDA - Digital Repository of the University of Helsinki

Muita tietoja – Övriga uppgifter – Additional information

List of abbreviations

A – adenosine

ac^4C_m – *N4*-acetyl-2'-*O*-methylcytidine

Ala – alanine

APS – ammonium persulfate

BCP – 1-bromo-3-chloropropane

bp – base pairs

C – cytidine

cDNA – complementary DNA, synthesized from a single-stranded RNA template

CFPS – cell-free protein synthesis system

CFU – colony forming units

cm^5U – 5-carboxymethyluridine

D – dihydrouridine

ddH_2O – double distilled water

DMSO – dimethyl sulfoxide

DNA – deoxyribonucleic acid

DTT – dithiothreitol

E – glutamic acid

EB – elution buffer

EDTA – ethylenediaminetetraacetic acid

ELP1 – Elongator Acetyltransferase Complex Subunit 1

EqB – equilibrium buffer

ESI – electrospray ionization

E-site – exit, empty tRNA site of the ribosome

G – guanosine

g – relative centrifugal force

GFP – green fluorescent protein

H_2O_2 – hydrogen peroxide

hm^5C – 5-hydroxymethylcytidine

ht^6A – hydroxy-*N6*-threonylcarbamoyladenosine

I – inosine

IVT tRNA – *in vitro* transcribed tRNA

Leu – leucine

Log – logarithm

LSU – large subunit of the ribosome

Lys, K – lysine

m/z – mass-to-charge ratio

m^1G - *N1*-methylguanosine

$m^1\Psi$ – 1-methylpseudouridine

$m^{2,2,7}G$ – *N2*,*N2*,7-trimethylguanosine

m^5D – 5-methyluridine

$m^{6,6}A_m$ – *N6*,*N6*,2'-*O*-trimethyladenosine

m^6A – *N6*-methyladenosine

mcm^5U – 5-methoxycarbonylmethyluridine

mRNA – messenger RNA

MS – mass spectrometry

NAIL-MS – nucleic acid isotope labeling coupled mass spectrometry

NaOAc – sodium acetate

ncs2 – gene for Cytoplasmic tRNA 2-thiolation protein 2

nt – nucleotides

O/N – overnight

OD_{600} – optical density at 600 nm

OHyW – hydroxywybutosine

OHyWy – methylated undermodified hydroxywybutosine

PAA – polyacrylamide

PAGE – polyacrylamide gel electrophoresis

P-site – peptidyl tRNA site of the ribosome

PTC – peptidyl transferase center

PTM – post-transcriptional modification

Q – glutamine

Rat1 – nuclear 5' to 3' single-stranded RNA exonuclease of yeast

rDNA – genes encoding ribosomal RNA

RNA – ribonucleic acid

RNase P – ribonuclease P

rpm – revolutions per minute

rRNA – ribosomal RNA

RT – room temperature

s^2U – 2-thiouridine

SDS – sodium dodecyl sulfate

snoRNA – small nucleolar RNA

SSU – small subunit of the ribosome

T – thymidine

t^6A – *N6*-threonylcarbamoyladenosine

TBE – Tris/Borate/EDTA buffer solution

TEMED – N, N, N', N'-tetramethylene-diamine

TES solution – Tris HCl (pH 7.5), EDTA and SDS solution

TFA – trifluoroacetic acid

tRF – tRNA-derived fragment

tRNA – transfer RNA

tRNA-Seq – tRNA sequencing

Tyr – tyrosine

U – uridine

U_{34} – uridine at wobble position of anticodon

UPLC/MS – ultra performance liquid chromatography coupled mass spectrometry

URM1 – Ubiquitin-related modifier-1

V – uridine-5-oxyacetic acid

WB – wash buffer

YPD – yeast extract-peptone-dextrose yeast growth medium

yW – wybutosine

yW-58 – 7-aminocarboxypropylwyosine methyl ester

yW-72 – 7-aminocarboxypropylwyosine

yW-86 – 7-aminocarboxypropyl-demethylwyosine

Ψ – pseudouridine

Contents

1. Introduction

1.1. Transfer RNA

Transfer RNA (tRNA) has a key role in translation, as carrier of the amino acid to the ribosome and messenger RNA (mRNA). Genes for tRNAs are numerous and scattered throughout the genome as multiple repeated sequences, example being *Saccharomyces cerevisiae* where 274 tRNA genes are scattered throughout the 16 chromosomes (Haeusler *et al.* 2008). They are transcribed by RNA polymerase III to pre-tRNA and maturation consists of several major steps: (1) removal of the 5' leader by RNase P, (2) removal of the 3' trailer sequence by a combination of endonucleases and exonucleases; (3) addition of CCA in eukaryotes; (4) splicing of introns in some tRNAs of most eukaryotes and some archaea; and (5) numerous modifications of tRNA at multiple residues (Hopper & Phizicky, 2003).

Mature tRNA lengths vary about 70-100 nt and the structure is well known. The secondary structure is known as the tRNA cloverleaf, as certain ribonucleotides form double-stranded stems and the others form single-stranded loops (Fig. 1.1). The anticodon which pairs complementarily to the codon on mRNA is located on the anticodon loop, whereas the amino acid carried by the tRNA is added to the 3' tail (CCA), close to the acceptor stem. Other loops are D-loop (named after dihydrouridine modification (D) present in this loop), TΨC-loop (named after the TΨC sequence present in this loop, specific due to the pseudouridine (Ψ) modification) and the variable loop.

The tertiary structure of tRNA is letter L shape (Fig. 1.1, upper left corner), where the tips are the anticodon and the acceptor stem (Watson, 2014). All domains of the tRNA are functionally important and interact with various molecules (Fig. 1.1), such as mRNA (anticodon), aminoacyl tRNA synthetases - enzymes which charge the tRNAs with the correct amino acids (anticodon loop and acceptor stem), and ribosomes (acceptor stem, anticodon loop and TΨC-loop).

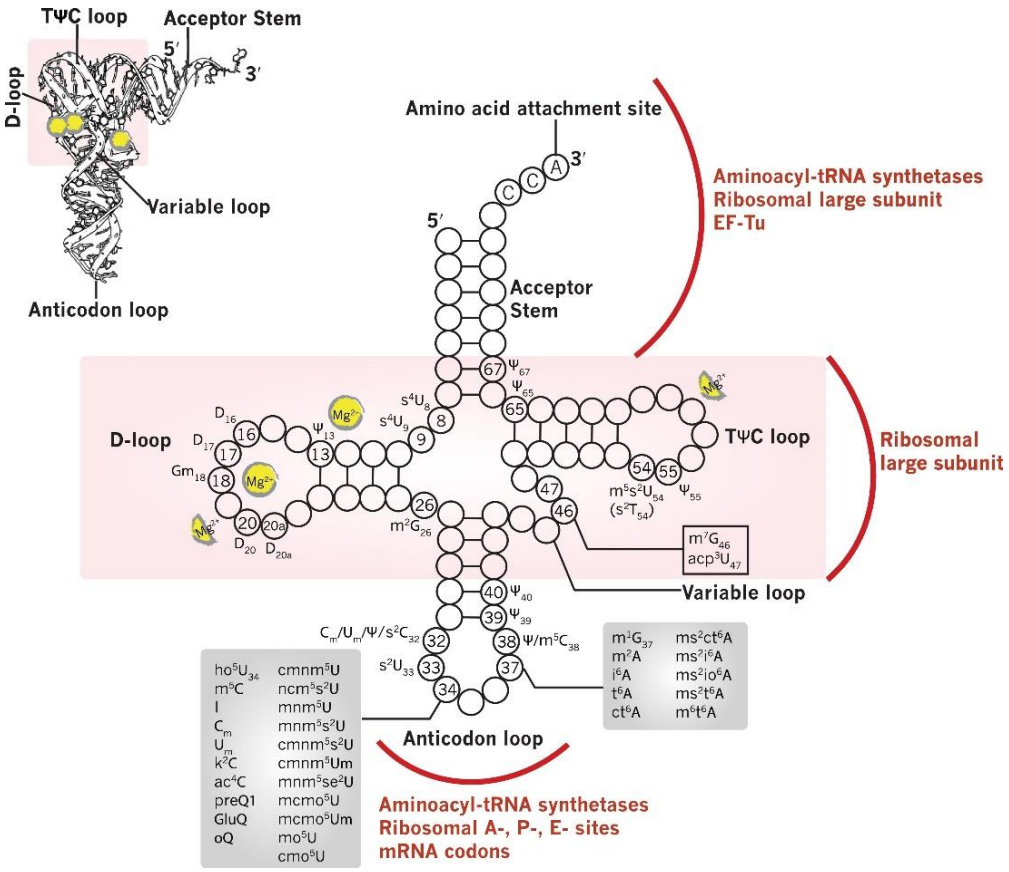

Figure 1.1. Schematic tRNA structure with known modifications and their positions indicated, reproduced with permission from Koh & Sarin, 2018

1.1.1. Post-transcriptional modifications in tRNA

Post-transcriptional modifications (PTMs) in tRNA are numerous and tRNA is known as the most highly modified RNA species (Machnicka *et al.* 2013). Modifications range from simple chemical modifications, like methylation or thiolation, to complex modifications for which several steps and enzymes are needed (Helm, 2006). They can be added co-transcriptionally, and free modified nucleosides are present in cells as well. Chemical alteration can happen in the base, at the ribose, or both and modified molecules can be found in intermediate modified states or the final hypermodified state (Iwata-Reuyl, 2008). One such modification is wybutosine, found at position 37 of phenylalanine tRNAs, known to be synthesized fully in 5 independent enzymatic reactions, each producing one modified state found in cells (Perche-Letuvée *et al.* 2014).

Modifications appear in nearly every position on tRNA, starting with the already mentioned D and Ψ in D and TΨC loops. Most diverse modifications are present in the

anticodon loop, particularly positions 34 (wobble position) and 37 are prone to modification (Koh & Sarin, 2018).

Essential roles of modifications are obvious when higher eukaryotes are considered. For example, even though deletion of *ELP1* gene (crucial for tRNA wobble uridine synthesis) in yeast shows subtle phenotypes, in mice the deletion of its homolog is lethal already in early embryonic stage (Sarin & Leidel, 2014; Chen *et al.* 2009). Perturbed tRNA modification leads to proteotoxic stress, which can lead to cell death. Although that may not affect the population of unicellular organisms, in a multicellular organism it leads to propagation of stress even among healthy cells or tissues, resulting in death especially at an embryonic stage. Due to that, it is crucial to consider growth and dynamics of modifications during stress conditions as well, in order to elucidate their roles, as fully characterizing them in multicellular organisms may not be feasible.

1.1.2. PTMs roles in tRNA structure and translation

tRNA function is in translation, as carrier of the amino acid incorporated correctly based on codon-anticodon complementary base pairing. For example, amino acid alanine (Ala) is encoded by 4 codons, all starting with GC: GCA, GCG, GCU, and GCC. Anticodons for Ala should then be complementary to those, except the third nucleotide can in fact be any of the 4 canonical nucleotides. So, in anticodon on tRNA, that "complementary" nucleotide can be a modified nucleotide which would enable non-Watson-Crick base pairing and enable pairing with several codons. This nucleotide is at the position 34 in the tRNA, it is known as the "wobble" position, and it is prone to being modified. Known alanine anticodons (Devi & Lyngdoh, 2018) in fact include the UGC (canonical, expected) and IGC (I = inosine) and VGC triplets (V = uridine-5-oxyacetic acid). Inosine pairs with U, A and C and V pairs with U, A, and G (Näsvall *et al.* 2007), so with these modifications, all codons are read.

Another example of that is the wobble uridine (U_{34}) universally modified to 5-methyl-2-thio derivatives in the tRNAs encoding for lysine, glutamine, and glutamic acid, namely tK^{UUU}, tQ^{UUG}, and tE^{UUC} (Rezgui *et al.* 2013). These modifications depend on active *ELP1* and *URM1* pathways (Noma *et al.* 2009, Leidel *et al.* 2009, Schaffrath & Leidel, 2017, Dauden *et al.* 2019, Pabis *et al.* 2020) and mcm^5 and s^2 groups were shown to improve reading of both A- and G-ending codons (Johansson *et al.* 2008).

Such non-standard base pairing can maintain Watson-Crick base pairing geometry (Demeshkina *et al.* 2012, Rozov *et al.* 2016) so that near-cognate tRNAs get recognized in addition to the cognate tRNAs. Result of these modifications is higher flexibility as all codons are read, and even in situation of the cell lacking certain ribonucleotide, translation can be rescued (Liu *et al.* 2016; Wang *et al.* 2018). Furthermore, virtually whole proteome integrity is thought to be maintained by tRNA modification at wobble uridine, as it is known that the ribosomes pause more frequently, and protein aggregates accumulate with loss of modifications on U_{34} (Nedialkova & Leidel, 2015).

It has been shown that modifications in tRNA (shown schematically in Fig. 1.1) have an impact on both function and structure of the tRNAs (Zhang *et al.* 2014, Piñeyro *et al.* 2014, Brandmayr *et al.* 2012, Helm, 2006). Some authors generally divide tRNA modifications into two families: those that may play a role in the codon-anticodon interaction at the decoding center of the ribosome and those that are likely to influence the structure of tRNA (Piñeyro *et al.* 2014), although such rigid divisions are often not biologically sound. Modifications in tRNAs are shown to affect the rigidity of the structure, some making tRNAs more rigid and some more flexible (Zhang *et al.* 2014). Modifications outside of the anticodon's wobble position are thought to play the crucial roles in stabilizing the tRNA structure, enabling the functions of the tRNAs and countless molecular interactions. Interactions with not only the mRNA (as shown in Ala codons/anticodons examples), but also with the aminoacyl-tRNA synthetases (Hibi *et al.* 2020) and ribosomal sites (potentially interacting with both ribosomal proteins and ribosomal RNAs) are known to be affected by the modifications in tRNAs.

Importance of tRNA modifications is evident, not only from the structural and functional impact they have, but also from the fact that many PTMs and enzymes associated with them are shown to be evolutionarily conserved (Koh & Sarin, 2018; Helm, 2006; Hopper & Phizicky, 2003). Modifications in tRNA have been quantified at a very fine scale and found to be linked to phylogenetic variation in studies with multiple species (Globisch *et al.* 2011). Conservation of tRNA modifications and enzymatic pathways is found in all 3 domains of life, and modifications like m^1G and $m^1\Psi$ have been proposed to have been present in ancient cells during evolution to improve reading frame maintenance (Björk *et al.* 2001).

1.2. Ribosomal RNA

Ribosomal RNA (rRNA) has a key role in translation, as structural and functional parts of ribosomes, together with numerous ribosomal proteins. rRNAs constitute the largest portion of the RNA molecules in cells (70-80%, Calo *et al.* 2015). Genes for rRNAs (rDNA) are present in over 100 copies in most eukaryotes and they are organized in clusters of tandem repetitive genes. For example, yeast *Saccharomyces cerevisiae* has 1 cluster on chromosome 12 with about 150 copies (Kobayashi *et al.* 1998), whereas human rDNA is in 5 clusters, each on separate chromosome and each containing about 70 copies (Sakai *et al.* 1995).

Eukaryotic rRNA types are 5S rRNA, transcribed by RNA Polymerase III independently from other rRNA types, and 18S, 5.8S and 25S rRNA (28S rRNA in humans for example), which are transcribed together by RNA Polymerase I into composite 35S rRNA precursor. Transcription of the 35S rRNA happens in the nucleolar part of the nucleus, and already transcribed 5S rRNA is transported to the nucleolus for assembly to ribosomal subunits (Eichler & Craig, 1994).

Maturation of 35S rRNA includes a series of endonucleolytic cleavage events, led by ribonucleoprotein complexes of snoRNA U3 (small nucleolar RNA U3) in association with numerous proteins (Watson, 2014, Eichler & Craig, 1994). All spacer regions cleaved out of the 35S rRNA are degraded exonucleolytically, in yeast by exonuclease Rat1 (Granneman *et al.* 2011). During processing of rRNA and later during assembly and export, ribonucleoside modifications at multiple residues are added, and it has been known since the first methylation maps were produced that modification patterns are non-random and conserved (Maden, 1988, Khan *et al.* 1978, Maden & Salim, 1974, Klootwijk & Planta, 1973).

1.2.1. Post-transcriptional modifications in rRNA

Ribosomal RNAs (rRNA) are universally modified, and PTMs are situated on specific, highly conserved residues, clustered at functionally important spots of the ribosome (Sharma & Lafontaine, 2015). In the small subunit (SSU), modifications in rRNA appear to be near the decoding site (site of mRNA placing and reading), and in the large subunit (LSU) they appear to be near the tRNA binding sites, ridges between P-(peptidyl tRNA) and E-sites (empty tRNA) and PTC (peptidyl transferase center). Given the fact that types and sites of modifications are conserved, it is likely that these modifications have been selected for and that they optimize the ribosomal structure and functions. Mostly methylations are known in rRNAs and they are

believed to be added in specific order which may serve as quality control steps in the biogenesis of the ribosome (Penzo & Montanaro, 2018, Sloan *et al.* 2017).

Approximately 2% of rRNA nucleotides get modified (Yang *et al.* 2016), which is less than in tRNA, but it appears that RNA modifications are intertwined together and the crosstalk between different classes of RNA and their modifications is essential. However, modifications in rRNA are less studied than in tRNA and determining modifications dynamics would be beneficial. Precise function of most modifications is still unknown, but evidence from various organisms shows that modifications are essential. In *Mollicutes* species that have drastically reduced their genome size during evolution, uridine thiolation (s^2U) was shown to be part of an essential core module of translation (Grosjean *et al.* 2014). Methylation pathways were also shown essential alongside thiolation, and pathway for the synthesis of t^6A (*N6*-threonylcarbamoyladenosine). Modifications are also found in viral RNAs (Gokhale & Horner, 2017), which all points towards the conclusion that RNA modifications are indispensable parts of the translation machineries. Although deletions of most rRNA modifications are not deleterious in eukaryotes (Sharma & Lafontaine, 2015), the modifications are of great importance for maintaining translation efficiency and accuracy.

1.3. PTMs in stress conditions

Many modifications are found to be redundant in physiological conditions, and their role is shown only in stress conditions. It is argued that the modification content of tRNA is a representation of the metabolic state of the cell (Koh & Sarin, 2018), and the functions of modifications in RNA have been observed during various stress responses.

One example is the generation of the mcm^5U_{34} which is required for wild-type tolerance to oxidative stress in *Schizosaccharomyces pombe* (Fernández-Vázquez *et al.* 2013). Translation during oxidative stress was found to be shifted to stress-related codon usage mRNAs. Mutants lacking the enzymes required for mcm^5U_{34} formation had inefficient translation, which was found to be rescued by overexpression of Lys tRNA (UUU) and by adding the modified uridine. Efficient translation during stress response was enabled by the modification presence, demonstrating its importance. In Rezgui *et al.* 2013, differences in protein levels between stress and control were minor but stressed cells did have impaired (slower) growth, again demonstrating the impact of mcm^5U_{34}.

Exposing yeast to hydrogen peroxide resulted in a specific increase in C_m, m^5C, and $m^{2,2}G$ modification levels (Chan *et al.* 2010). Besides oxidative stress, temperature stress is known to change the presence of tRNA modifications. In Alings *et al.* 2015, tRNA modification levels were defined for 6 yeast species in response to elevated temperatures. 2-thiolation at wobble uridine was found to be high at high temperatures, due to mutation in *ncs2* gene which conveys enzyme functionality at elevated temperatures. Furthermore, yeast species without U_{34} modifications were found to be sensitive to high temperatures and chemical stress. Mutation at *ncs2* was found to be common in wild and pathogenic yeast strains, exemplifying how studying only common laboratory strains cannot elucidate the full genotypic and phenotypic variation in nature.

Nutrient deprivation stress in *Saccharomyces cerevisiae* was also shown to affect tRNA modifications (Laxman *et al.* 2013), resulting in the discovery that thiolation amounts are tuned to reflect intracellular sulfur amino acid availability. In stressful growth conditions, fine-tuning tRNA thiolation appears to be essential as it is related to amino acid and carbohydrate metabolism.

Many of the modifications have been also shown to change in presence/abundance as a response to stress conditions (Alings *et al.* 2015). Certain modifications are even unique to stress conditions (reviewed in Koh & Sarin, 2018) and it is of interest to know the impact on translation. During stress, translation needs to be efficient and optimized for the cells to survive, especially translation of stress-response proteins, so it is hypothesized that stress-related modifications may play a crucial role in continuing correct and optimized protein synthesis during cellular stress response (Koh & Sarin, 2018). Stress-response translation is known to be preferential for stress-response proteins while the translation of general proteins decreases (Holcik & Sonenberg, 2005).

Although the impact of the stressors on tRNA modifications is clear, it is still not confirmed whether the tRNA modifications dynamic is a result of active or passive adaptation. It is likely that a combination of mechanisms is behind it, as there is a multitude of enzymes involved in modification and de-modification, as well as a multitude of interactions involving modified nucleosides of the tRNAs.

In rRNA, precise function of most modifications is still unknown, but cells which lack certain modifications (due to deletion or knock-down of relevant proteins) have been shown to be outcompeted by wild-type cells (Sharma & Lafontaine, 2015). They also show increase in

stress sensitivity and are correlated with multiple diseases and cancer in humans (McMahon *et al.* 2015).

Within cells, there can be differentially modified ribosomes, which is evidence fueling the idea of specialization of certain ribosomes (Gilbert, 2011, Lafontaine, 2015, Ferretti & Karbstein, 2019) and partially modified (sub-stoichiometric modification) rRNAs were found upon stress experiments dealing with nutritional stress (Sloan *et al.* 2017). As modifications in rRNA are less studied than in tRNA, determining the biological consequences of ribosome specialization and rRNA differential modification during physiological and stressful conditions would be beneficial.

2. Study aims

Post-transcriptional modifications (PTMs) in RNA are present in all known RNA species and conserved in all kingdoms of life (Kim *et al.* 2010; Gokhale & Horner, 2017; Koh & Sarin, 2018). Similarly to epigenetic modifications present in DNA, modifications in RNA species have been collectively termed epitranscriptome. Epitranscriptomics has been field of interest in the recent years, considering the discoveries of modifications roles in translation, infection and disease (Song *et al.* 2020; Koh & Sarin, 2018; Liu *et al.* 2016). Extensive efforts have been made in establishing protocols and new approaches for high-throughput identification and quantification of RNA modificome (Zhang *et al.* 2020, Gregorová *et al.* 2020).

PTMs have been shown to change during stress conditions in RNAs and to influence translation in various ways previously mentioned. In line with that, this master's thesis project sought to gain insight into the dynamics of PTMs in tRNA and rRNA upon oxidative stress, with the goal of utilizing recently optimized UPLC/MS method (Gregorová *et al.* 2020) for identifying modified ribonucleosides, while laying the foundation to study the evolutionary conserved function of PTM changes during stress as modulators of translation.

As the specific aim of the thesis was to estimate the change in PTMs in tRNA and rRNA in response to oxidative stress with 0.5 mM and 2 mM hydrogen peroxide H_2O_2, 3 immediate goals were set: (i) to isolate total tRNA from yeast grown in stress conditions, (ii) to isolate rRNA from yeast 80S ribosomes, and (iii) to identify present modifications using mass spectrometry.

3. Materials and methods

The chemicals used were purchased from Acros Chemicals and/or Fisher Chemicals in highest purity level available, unless otherwise stated. The overview of experimental design is shown in the Fig. 3.1 and details of each method are explained below.

3.1. Yeast cultures

Yeast was cultured in Yeast Extract-Peptone-Dextrose, YPD medium (exact recipe in Table 1). *Saccharomyces cerevisiae* BY4741 culture was started by streaking yeast stock material (kept at -80°C) with a sterile wooden toothpick onto plates with solid YPD, and incubated at 28°C. From starter plates, yeast was transferred into liquid YPD using sterile toothpick to grow overnight (O/N) at 28°C, 180 rpm. To enable good and even aeration, the culture volume did not exceed 1/5 of the maximum volume of the Erlenmeyer flask. Main cultures were started using O/N culture with an $OD_{600} \approx 0.2$ (optical density at 600 nm), by diluting the O/N cultures appropriately.

Table 1. Yeast Extract-Peptone-Dextrose (YPD) medium (liquid or solid)

Reagent	Quantity
Yeast extract	10 g
Peptone	20 g
Dextrose	20 g
Agar (for solid medium)	20 g
Dissolve reagents in 1 L of didistilled water. Autoclave for 20 min at 121°C and 0.5 bar. Store at room temperature.	

Cells were harvested by centrifugation for 10 min at 6000 *g*, 4°C, discarding the supernatant and snap-freezing the pellet in liquid nitrogen. Cells were washed in 1-2 mL ice-cold ddH_2O to avoid YPD leftover interference with downstream analyses, re-centrifuged and the pellet was frozen in liquid nitrogen. Frozen cells were kept in temperature -80°C until the start of RNA isolation.

For cultures used for ribosome and rRNA isolation, translation was arrested by adding cycloheximide (stock prepared as 100 mg/mL solution in DMSO) in final concentration of

0.1 mg/mL and then cells were pelleted. The cell pellets were resuspended in Ribo Lysis Buffer (Table 3) using 1 mL of the buffer per 1 g of cell pellet, and then frozen in liquid nitrogen by pipetting droplets into a pool of liquid nitrogen.

3.2. Oxidative stress experiments

Yeast cultures were started at OD_{600} = 0.2 from O/N cultures in triplicate for each treatment (Figure 3.1). Treatments used were the following: 0, 0.5, 2.0 mM hydrogen peroxide (H_2O_2), solutions were prepared fresh with YPD medium right before elicitation. Two treatments were chosen to induce sublethal stress and therefore reflect physiological range of oxidative stress that the cells might encounter in nature. Elicitation was done at OD_{600} = 0.4-0.5, before which t_0 time point was plated (plating was done with dilutions 10^{-4} and 10^{-5} by plating 100 µL of the diluted culture) and 100 mL culture was harvested for downstream analyses by centrifugation and snap-freezing the cell pellets in liquid nitrogen, as previously described (section 3.1.).

Other collection time points were t_1 and t_2, 2 and 24 hours after elicitation (plating done with dilutions 10^{-4}, 10^{-5} and 10^{-6} by plating 100 µL of the diluted culture; 100 mL culture harvested for downstream analyses by centrifugation and snap-freezing the cell pellets in liquid nitrogen, as previously described). Plates were incubated for about 48 hours at 28°C and then colonies were counted to calculate the colony forming units (CFU) or the number of viable cells per milliliter (formula below).

$$CFU/mL = \frac{number\ of\ colonies\ on\ the\ plate}{Volume\ plated\ [mL] \times Dilution\ Factor}$$

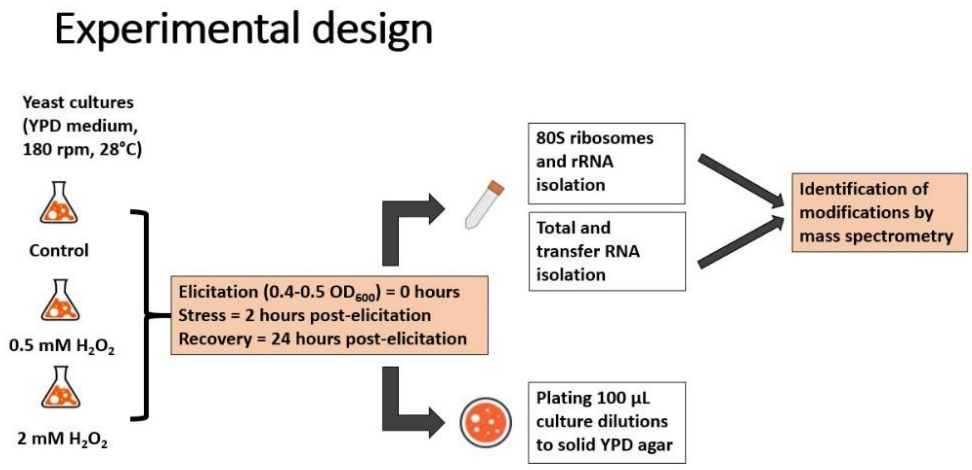

Figure 3.1. Experimental design of the oxidative stress experiment. Yeast cultures were treated with 0.5 mM and 2 mM H_2O_2 at mid-logarithmic growth phase (OD_{600} = 0.4-0.5), and control cultures were not treated. Cells for RNA isolation were harvested at elicitation time, 2 and 24 hours later. OD_{600} and cell viability assay was done at all three time-points to determine the treatment impact on culture growth. Experiment was repeated with three independent biological replicates and within each experiment cultures done in duplicate.

3.3. Total and tRNA isolation

Isolation of total RNA from frozen cell pellets was performed using the hot phenol method as previously described in Collart & Oliveiro, 1993 and adapted by Minna-Maria Heinonen (personal communication). List of chemicals used in this protocol is available in Table 2. Briefly, this is an RNA isolation method based on acidic phenol (pH 4.3) heated to 65°C, and 1-Bromo-3-chloropropane (BCP) and precipitation using 100% ethanol (or isopropanol).

Cells pelleted from 100 mL cultures were first thawed, and 5 mL TES solution was added (Table 2). Then 5 mL pre-heated phenol is added and the lyzed cell pellets are incubated at 65°C for 1 hour before proceeding to add 1 mL BCP. For efficient RNA isolation, occasional vortexing can be done during the 1-hour incubation at 65°C. After incubation, phase separation is done by centrifugation for 15 min at 10000 *g*, at room temperature (RT). The aqueous phase on top of the inter- and organic phase contains RNA, which was then re-isolated twice by addition of 4 mL acidic phenol in the first aqueous phase, and 2 mL BCP in the second. The suspension is vortexed and centrifuged for 15 min at 10000 *g* in each re-isolation step and the aqueous phase is collected into fresh tubes. The final aqueous phase is precipitated using

sodium acetate (pH 5.3, to final concentration 300 mM) and ice-cold 100% ethanol (2.5× volume of the collected aqueous phase). Precipitated RNA is pelleted by 20 min centrifugation at 10000 *g*, 4°C, washed repeatedly by vortexing in ice-cold 70% ethanol until clean. Pellet is then air-dried and resuspended in 100 µL ddH_2O.

Table 2. Buffers and chemicals used for total RNA isolation from yeast cultures by hot phenol method

	Components	**Final concentration**
TES solution	Tris HCl (pH 7.5)	10 mM
	Ethylenediaminetetraacetic acid, EDTA	10 mM
	Sodium dodecyl sulfate SDS	0.5%
Acidic phenol (citric acid buffered pH 5.3)		
1-bromo-3-chloropropane, BCP		
Sodium acetate NaOAc (pH 5.3)		300 mM
Ethanol, ice-cold		70%

From isolated total RNA, total tRNA was isolated using anion exchange chromatography method with Nucleobond AX-100 solid-phase cartridge column (Macherey-Nagel). Column was equilibrated with buffer Eq (with Triton X-100, 10 mL, Table 3). Then 100 mg of total RNA in 10 mL buffer Eq (no Triton X-100) was applied onto the column. Column-bound RNA was washed then with wash buffer WB (5 mL, Table 3), and then eluted with elution buffer EB containing increasing concentration of KCl, 700 mM, 750 mM or 800 mM respectively (5 mL each, Table 3). Buffers WB and EB were heated to 55°C beforehand. To all collected fractions at least 2.5× volume 100% ethanol was added, and tRNA was then precipitated overnight at -20°C. Precipitate was pelleted by centrifugation at 10000 *g*, 4°C for 30 min, and salt was subsequently washed out with 80% ethanol. The final tRNA pellet was air-dried at room temperature and re-suspended in 20 µL ddH_2O. All equipment and working spaces were kept clean with 3% hydrogen peroxide to inhibit RNase which would compromise the RNA isolation.

Table 3. tRNA isolation buffers; EqB is equilibration buffer, WB is wash buffer and EB is elution buffer, ddH_2O is double distilled water

	Stock	EqB	WB	EB	0.9% NaCl
Chemical	conc.	conc.	conc.	conc.	
Tris (pH 6.3)	1 M	10 mM	10 mM	10 mM	
Ethanol	99.6%	15%	15%	15%	
KCl	3 M	200 mM	300 mM	700 mM / 750 mM / 800 mM	
Triton X-100	10%	0.15%			
ddH_2O					31.5 ml
NaCl	5 M				1 ml

3.4. RNA concentration and quality check by gel electrophoresis

To check the presence and quality of isolated total RNA, NanoDrop and gel electrophoresis was used. NanoDrop was used to estimate the concentration and quality of the isolated RNA as indicated by the ratios of absorbance A_{260}/A_{280} (≈2.0 for pure RNA) and A_{260}/A_{230} (2.0-2.2 for RNA).

Denaturing urea polyacrylamide gel electrophoresis (PAGE) was done, using 10% polyacrylamide (0.5× TBE as running buffer) to visualize smaller RNA species, e.g. tRNAs (run both for total RNA and tRNA). As a size marker for the detect RNAs GeneRuler Low Range DNA Ladder (Thermo Scientific™) was used. RNA (500-1000 ng for total RNA gels, and 100-200 ng for tRNA gels) was loaded with 2 × formamide loading buffer (90% formamide, 0.5 × TBE, 0.025% bromophenol blue, 0.01% xylene cyanole FF, 0.05% SDS) and denatured for 5 min at 98°C. Electrophoresis was run for 90 min at 180 V, and then stained with 1× SYBR™ Gold (from 10000 × stock, Invitrogen) in 0.5 × TBE by incubating for 5 min with shaking.

To check the presence and quality of isolated rRNA, 1% agarose gel (TBE, 1× TBE as running buffer) electrophoresis was used, alongside concentration determination with NanoDrop. Midori Green was used for staining the agarose gel (1.5 µL / 100 mL gel) and 500-1000 ng RNA isolate was loaded into the gel. RNA was loaded with 1.5 × formamide loading buffer (90% formamide, 1× TBE, 0.025% bromophenol blue, 0.01% xylene cyanole FF) after denaturing in 80°C for 5 min and 1 kb DNA ladder was used as size reference (GeneRuler 1 kb DNA Ladder, Thermo Scientific™). Electrophoresis was run for 60 min in 75 V. Visualization of the gels was done with Bio-rad ChemiDoc™ Touch Imaging System gel imager.

3.5. Ribosome and rRNA isolation

Ribosome purification was done using protocol adapted from Acker *et al.* (2007). Briefly, purification of ribosomes is based on ultracentrifugation of cleared yeast cell lysate in sucrose cushion. This approach is used with 1 M sucrose in the sucrose cushion, which is equal to 33% sucrose solution and density of 1.12-1.18 g/cm^3 and allows for 80S ribosomes separation upon ultracentrifugation. As the ribosomes are denser than the sucrose cushion, they are pelleted down by ultracentrifugation, whereas other cell components that are not as heavy stay above the cushion.

Cell lysates are obtained by adding Ribo Lysis buffer, 1 mL per 1 g of cell pellet, (Table 4) to the samples cell pellets from yeast cultures and kept at -80°C after freezing with droplets of liquid nitrogen. Samples are thawed and then French pressed (at least twice to lyse the whole sample). To clear the samples from cellular debris samples are then centrifuged for 15 min at 10000 *g*, 4°C and 2 mL supernatant is pipetted onto 3 mL sucrose cushion (Table 4) prepared in tubes for ultracentrifugation. Volumes of the cell lysate and sucrose cushion were calculated so that they fill 2/3 of the ultracentrifuge tubes for fixed angle rotor used (Thermo Scientific T-1270 Titanium rotor, 24° fixed angle). Prepared samples are then ultracentrifuged for 212 min at 109850 *g*, 4°C (Sorvall™ wX+ Ultra Series centrifuge, Thermo Scientific). Ribosomes formed glass-clear pellets and the supernatant was discarded. Pellets were dissolved in 1 mL Ribosome extract buffer (Table 4).

Table 4. Ribosome purification buffers, as recommended in Acker *et al.* 2007; 10x Ribo Buffer A is made from 200 mM Hepes · KOH, pH 7.4; 1 M KOAc, pH 7.6; 25 mM $Mg(OAc)_2$

	Ribo Lysis Buffer	**Sucrose Cushion**	**High Salt Wash**	**Ribosome Sucrose Storage Buffer**	**Ribosome Extract Buffer**
Chemical	Concentration				
10x Ribo Buffer A	1×	1×	1×	1×	
Heparin	1 mg/ml		1 mg/ml		
Dithiothreitol, DTT	2 mM	2 mM	2 mM	2 mM	
Protease inhibitor tabs	+				
AEBSF	0.5 mM				
KCl		500 mM	500 mM		
Sucrose		1 M		250 mM	
NaOAc (pH 5.0)					0.3 M
EDTA					12.5 mM
SDS					0.5%

From the purified ribosomes, ribosomal proteins (r-proteins) and ribosomal RNA (rRNA) were isolated. Proteins were isolated by adding 4 volumes acetone with 20 mM dithiothreitol (DTT), vortexing and then incubating at -20°C overnight. Following day, samples were centrifuged at 10000 *g*, 4°C for 15 min, supernatant was discarded and the pellet dried. The purification result was checked by SDS-PAGE (Sodium Dodecyl-Sulfate PolyAcrylamide (PA) Gel Electrophoresis) with 10% PA separation gel and 4% PA stacking gel (Table 6). Samples were loaded with 2× SDS-PAGE Loading buffer (4% (w/v) SDS, 20% glycerol, 120 mM Tris-HCl (pH 6.8, and 0.02% (w/v) bromophenol blue) and denatured for 10 min at 98°C before loading into the gel. Gel was run first at 70 V for about 15 min, and then for 1 hour at 90 V. Gel was stained with Coomassie Blue solution (2% alpha-cyclodextrin, 0.3% 2-hydroxyethylcellulose, 5% orthophosphoric acid, 2% ethanol, and 0.0045% Coomassie G250) by incubating for 10 min with shaking. As reference, PageRuler Plus Prestained Protein Ladder was used (10 to 250kDa, loading 5µL, Thermo Scientific Fisher Scientific).

Table 5. Protein separation gel recipe (SDS-PAGE, Sodium Dodecyl-Sulfate Polyacrylamide Gel Electrophoresis)

Separation gel (10%)	
ddH_2O	8.82 mL
Acrylamide/bis (40%)	4.5 mL
Tris-HCl (1.5 M, pH 8.8)	4.5 mL
SDS, 10%	180 µL
N, N, N',N'-tetramethylene-diamine (TEMED)	18 µL
Ammonium persulfate (APS), 10%	57.6 µL
Stacking gel (4%)	
ddH_2O	6.4 mL
Acrylamide/bis (40%)	1 mL
Tris-HCl (0.5 M, pH 6.8)	2.5 mL
SDS, 10%	100 µL
N, N, N',N'-tetramethylene-diamine (TEMED)	10 µL
Ammonium persulfate (APS), 10%	100 µL

The rRNA were isolated from the purified ribosomes, using previously described phenol/BCP/ethanol method (see section 3.3). The isolation result was checked with NanoDrop and electrophoresis (agarose and polyacrylamide gels) as described previously (section 3.4).

3.6. Mass spectrometry preparation

Dephosphorylated mononucleosides for MS analysis were generated as previously described in Gregorová *et al.* 2020, Alings *et al.* 2015 and Leidel *et al.* 2009. Digestion of the transfer and ribosomal RNA (3-15 µg RNA material) into dephosphorylated mononucleosides was done enzymatically with Nuclease P1 (from *Penicillium citrinum*, Sigma-Aldrich) and alkaline phosphatase FastAP (Thermo Scientific). These enzymes were prepared as 1:10 dilutions, nuclease P1 diluted in 200 mM sodium acetate (pH 5.5) and FastAP diluted in ddH_2O, and the RNA samples were adjusted to volume of 19.8 µL by concentrating in Savant SpeedVac concentrator (Thermo Scientific). Each reaction was done in volume of 30 µL (19.8 µL RNA sample and 10.2 µL master mix, components of the master mix shown in Table 6). Procedure included 1.5-hour incubation followed with addition of 15 µL 0.5 M ammonium bicarbonate and 1 hour more of incubation. After that, the reaction was terminated by the addition of 5 µL 5% trifluoroacetic acid TFA (in water) and then by dilution of TFA to concentration of 1% by adding appropriate amount of 0.1% TFA (in water).

Table 6. Master mix for RNA digestion into dephosphorylated nucleosides, for 1 reaction

Solution	Volume (µL)
200 mM NaOAc, pH 5.5	3.0
Nuclease P1 (1:10 dilution)	3.2
FastAP (1:10 dilution)	2.0
50 mM $ZnCl_2$	2.0

Next step was purification of nucleosides using HyperSep HyperCarb Spin Tips (Thermo Scientific). The tips were first equilibrated using 0.1% TFA in water and micro centrifuging for 30 seconds at 845 *g* (this step is repeated 5 times, using 50 µL each time). Then the samples were applied and centrifuged using same conditions, washed 5 times with 50 µL 0.1% TFA in water and centrifuged. The nucleosides were eluted from the spin tips using 50 µL 0.1% TFA in 80% acetonitrile and centrifuging (repeated twice), while collecting the flow-through in a new 1.5 mL tube. Finally, the samples were dried out fully using Savant SpeedVac concentrator (Thermo Scientific) and resuspended in 11 µL 5 mM ammonium format (pH 5.3). The concentration and yield of nucleosides was checked using NanoDrop, where indication of successful cleavage was the shift of absorption peak from typical 260 nm for nucleic acids, to 255 nm typical for nucleosides. Following that, volumes of the samples

were adjusted by adding more 5 mM ammonium formate (pH 5.3) so the final concentrations of all samples were 80 ng/µL and 100 ng/µL, for tRNA and rRNA samples, respectively.

3.7. Mass spectrometry UPLC-MS

The presence of post-transcriptional modifications in sample RNA was assessed by mass spectrometry, as explained in detail in Gregorová *et al.* 2020. Analysis was done with Waters Acquity® UPLC system (Waters, Milford MA, USA) attached to Waters Synapt G2 HDMS mass spectrometer (Waters, Milford MA, USA) via an ESI ion source. Ribonucleosides from the yeast culture samples were loaded in volumes of 10 µL, so for tRNA samples loading amount was 800 ng and for rRNA samples 1000 ng. A standard mix was loaded before the experimental samples, including following 50 ribonucleosides: A, U, C, G, Ψ, A_m, U_m, C_m, G_m, s^2U, s^4U, mcm^5U, ac^4C, m^1G, m^2G, m^7G, m^1A, m^6A, m^3C, m^5C, m^3U, m^5U, ac^6A, ac^4C_m, ncm^5U, cm^5U, cnm^5U, imG-14, $m^{2,8}A$, $m^{4,4}C$, $m^{2,2}G$, $m^{2,7}G$, $m^{1,3}Ψ$, f^5C, hm^5C, ho^5U, I, mcm^5s^2U, mo^5U, m^8A, m^4C, m^1I, I_m, m^6A_m, m^4C_m, m^5C_m, $m^1Ψ$, m^5s^2U, ms^2m^6A, s^2C. Full names and masses are listed in Table 7. Separation was done using Acquity UPLC® Ethylene Bridged Hybrid [BEH] C18 columns (Waters, Ireland). Samples were analyzed in positive ion mode with the mass range (*m/z*) from 100 to 600.

Table 7. List of ribonucleosides used in the mix of standards for UPLC/MS. Masses of the ions which yield the strongest signal recorded by the detector are shown in bold. Standards were run separately in 4 mixes to differentiate isomeric modifications and then run also all 50 combined into a complex mix (as explained in detail in Gregorová *et al*. 2020).

Full name	Abbreviation	Monoisotopic mass	Product ions masses
adenosine	A	267	**268**, 136
uridine	U	244	245, **113**
citidine	C	243	244, **112**
guanosine	G	283	284, **152**
pseudouridine	Ψ	244	386, 264, 245, **209**, 191, 179, 155
2'-***O***-methyladenosine	A_m	281	**282**, 136
2'-***O***-methyluridine	U_m	258	259, **113**
2'-***O***-methylcytidine	C_m	257	515, 258, **112**
2'-***O***-methylguanosine	G_m	297	595, 298, **152**
2-thiouridine	s^2U	260	559, 427, 283, 261, **129**
4-thiouridine	s^4U	260	540, 410, 283, 261, **129**
5-methoxycarbonylmethyluridine	mcm^5U	316	494, 317, **185**, 153, 125
N4-acetylcytidine	ac^4C	285	571, 447, 286, **154**, 112
N1-methylguanosine	m^1G	297	298, **166**
N2-methylguanosine	m^2G	297	298, **166**
N7-methylguanosine	m^7G	297	298, **166**
N1-methyladenosine	m^1A	281	**282**, 150
N6-methyladenosine	m^6A	281	**282**, 150
*N*3-methylcytidine	m^3C	257	258, **126**
5-methylcytidine	m^5C	257	515, 258, **126**
N3-methyluridine	m^3U	258	407, 278, 259, **127**
5-methyluridine	m^5U	258	407, 278, 259, **127**
N6-acetyladenosine	ac^6A	309	310, **178**, 136
N4-acetyl-2'-*O*-methylcytidine	ac^4C_m	299	599, 300, **154**, 112
5-carbamoylmethyluridine	ncm^5U	301	471, **302**, 170, 153, 125
5-(carboxymethyl)uridine	cm^5U	302	473, 303, **171**, 153, 125
5-(cyanomethyl)-uridine	cnm^5U	283	586, 444, 284, **152**
4-demethylwyosine	imG-14	321	322, **190**
2,8-dimethyladenosine	$m^{2,8}A$	295	**296**, 164
N4,N4-dimethylcytidine	$m^{4,4}C$	271	272, **140**
N2,N2-dimethylguanosine	$m^{2,2}G$	311	312, **180**
*N2,*7-dimethylguanosine	$m^{2,7}G$	313	312, **180**
1,3-dimethylpseudouridine	$m^{1,3}Ψ$	272	428,292,273,**237**,219,207,183,153
5-formylcytidine	f^5C	271	543, 272, **140**
5-hydroxymethylcytidine	hm^5C	273	547, 272, **142**, 124
5-hydroxyuridine	ho^5U	260	540, 410, 261, **129**
inosine	I	268	537, 269, **137**
5-methoxycarbonylmethyl-2-thiouridine	mcm^5s^2U	332	518, 333, **201**, 169, 141
5-methoxyuridine	mo^5U	274	568, 431, 275, **143**
8-methyladenosine	m^8A	281	**282**, 150
N4-methylcytidine	m^4C	257	515, 258, **126**
N1-methylinosine	m^1I	282	565, 283, **151**
2'-*O*-methylinosine	I_m	282	565, 283, **137**
N6-methyl-2'-*O*-methyladenosine	m^6A_m	295	**296**, 150
N4-methyl-2'-*O*-methylcytidine	m^4C_m	271	543, 272, **126**
2'-*O*-methyl-5-methylcytidine	m^5C_m	271	543, 272, **126**
1-methylpseudouridine	$m^1Ψ$	258	407, 278, 259, **223**, 193, 169, 139
5-methyl-2-thiouridine	m^5s^2U	274	275, **143**
2-methylthio-N6-methyladenosine	ms^2m^6A	327	**328**, 196
2-thiocytidine	s^2C	259	260, **128**

3.8. Data analysis

Growth curve data was analyzed using R (version 4.0.4). Curves were plotted using ggplot2 package, using custom scripts calculating also means, standard deviations and errors.

MS raw data was analyzed using MZmine2 software (version 5.3) to generate total and extracted ion chromatograms (Katajamaa *et al.* 2006, Pluskal *et al.* 2010, Myers *et al.* 2017). Peaks were identified by using a custom lookup list of known ribonucleosides (courtesy of Pavlína Gregorová based on data from RNA modifications database MODOMICS, Boccaletto *et al.* 2018), and retention time identified from standards. Based on the data obtained, the list was further manually curated and additional ions identified in standards and biological samples were added.

For quantification, absolute intensities were normalized to cytidine (a canonical nucleoside, ion 112 used for tRNA samples and 244 for rRNA samples). Normalization was done with a canonical base for which the signal intensity is within the linear detection range of the instrument, ensuring that relative changes can be identified, and bias is not introduced to the data because the normalization ion appears static.

Relative changes presented as ratio of normalized intensities between treatment and control at each time-point (0.5 mM H_2O_2 / control, at t_1 and t_2; 2 mM H_2O_2 / control, at t_1 and t_2). For data visualization, the relative intensities were calculated for the ion of the most intense signal in the spectrum. Relative changes were calculated from mean of normalized peak intensities and plotted using ggplot2 package in R (version 4.0.4) and heatmap plotting in GraphPad Prism (version 9.0.0 for Windows, GraphPad Software, San Diego, California USA, www.graphpad.com). Example code used in R is available in the Supplement.

4. Results

4.1. Hydrogen peroxide impact on yeast growth and cell survival

To assess the effect of hydrogen peroxide treatments on yeast growth, OD_{600} and CFU/mL was measured. Treatments used here were 0.5 mM and 2 mM hydrogen peroxide, elicitating oxidative stress at mid-log phase (OD_{600} = 0.4-0.5). Representative growth curves from first replicate experiment are shown in Fig. 4.1, and growth curves from other two replicates are shown in the Supplement (Fig. S1 and S2). Figure 4.1A shows growth curve estimates as OD_{600} measurements and Figure 4.1 B represents cell viability measurement as CFU/mL. In both estimates, the effect of the treatments is visible as the decrease in growth at t_1, 2 hours upon stress elicitation. That effect on culture growth is not clear with 0.5 mM H_2O_2 treatment as the effect size appears small, but with 2 mM H_2O_2 treatment, higher effect size is seen and decrease in viable cell numbers is significant.

Results show clearly that cell survival is lower in the treatments than in the control (Fig. 4.1B). From these viable cell number estimates, the cell survival was estimated to be 58% and 16%, respectively (calculated as mean of experimental replicates). Furthermore, all cultures show a recovery after 24 hours as we see a high number of viable cells and no difference between the treatments and the control (Fig. 4.1B).

4.2. Analysis of total and transfer RNA isolated from peroxide stressed yeast cultures

In order to analyze tRNA modification, tRNA pools of all culture treatments needed to be isolated from total RNA. Total RNA isolation from 100 mL culture yielded between 650 µg and 14 mg RNA. RNA yield for all oxidative stress experiment samples is listed in Table 1. In addition to yield estimates from NanoDrop measurements, quality of isolated total RNA was checked on denaturing urea-PAGE and results are shown in Fig. 4.2 (replicate 3 presented; results of all replicates are shown in the Supplement, Fig. S3). As expected, in the total RNA gels there are signals of tRNA and ribosomal RNA (5S and 5.8S rRNA) and other RNA species are not visible due to their greater size. Negligible amounts of degradation are visible as smearing of the bands.

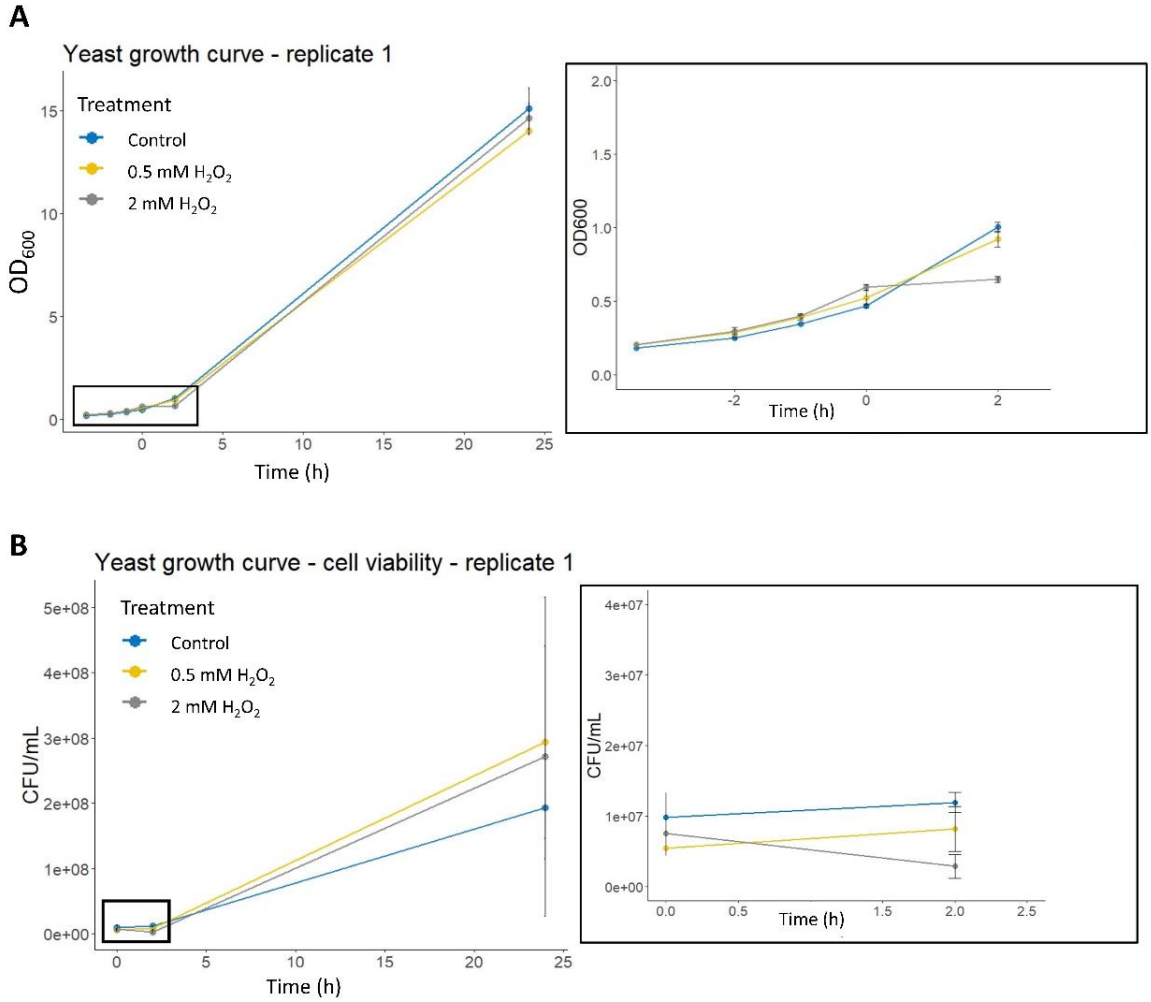

Figure 4.1. Yeast growth during oxidative stress. Panel A: OD_{600} measurements are plotted against time, on the left throughout the full experiment and on the right as a close-up for better visualization of time-points at elicitation and 2 hours after elicitation. Panel B: CFU/mL measurements are plotted against time on the left throughout the full experiment and on the right as a close-up for better visualization of time-points at elicitation and 2 hours after elicitation. Time is in hours, where 0 is the elicitation point, 2 is the stress point and 24 is the recovery (final) point. OD_{600} was measured hourly from 0.2 and those measurements are indicated with negative values of time. Dots represent mean of experiment duplicates and error bars represent the standard deviation.

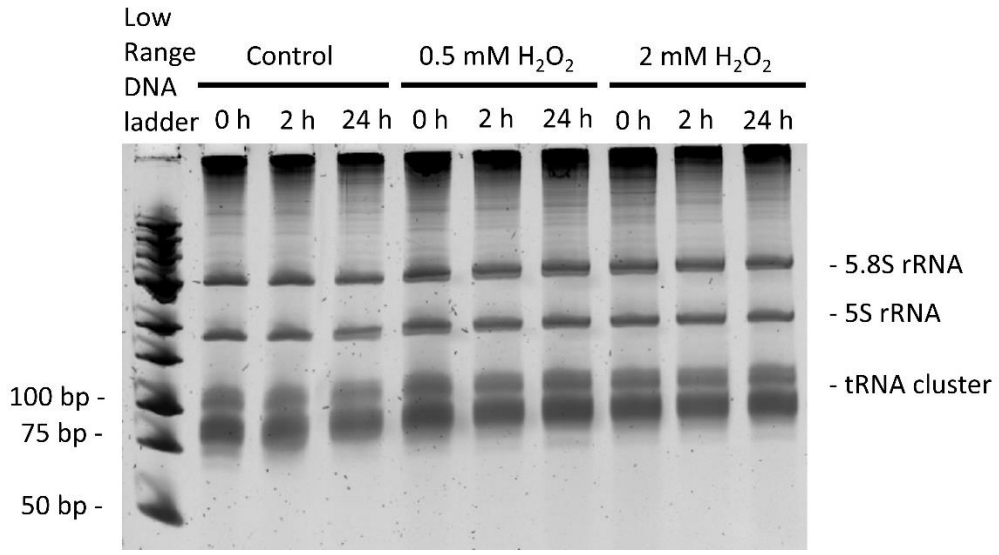

Figure 4.2. Total RNA quality check on denaturing urea PAA (10%) gel, one replicate presented. 500 ng RNA was loaded and stained with SYBR™ Gold. As size reference, Low Range DNA Ladder (Thermo Scientific™) was used.

tRNA pools were isolated using anion-exchange chromatography in order to analyze present modified ribonucleosides. Total yields are shown in Table 1. Due to the input requirements of the UPLC/MS analysis used here, a minimum yield goal of 5 µg was set initially. However, tRNA yields from both control and treatments were consistently below 5 µg. Consequently, multiple samples had to be re-isolated to ensure there was enough input material for the UPLC/MS analysis. Results of repeated isolations are included in the total yields shown in Table 1 (yields from all isolation repeats are available in the Supplement, Tables S1, S2 and S3). As the yields were sufficient only in 2 replicates, UPLC/MS analysis was done for them exclusively.

Regardless of low yields, when checked on polyacrylamide gels, most tRNAs were of good quality with clearly visible total tRNA cluster between 75 and 100 bp (result from replicate 1 shown in Fig. 4.3, results of all replicates are shown in the Supplement, Fig. S4). Several samples had visible degradation (smearing under the bands visible on gels), and contamination with 5S and 5.8S rRNA (121 and 158 nucleotides long, respectively) is visible in several samples, eluted with 800 mM KCl buffer.

Table 1. Total RNA and transfer RNA isolation yields for control and two treatments, for each of the 3 analyzed timepoints (at hours 0 = elicitation, 2 = stress, 24 = recovery) and all 3 replicates. *Total yield after 1 or 2 isolations

Treatment	Timepoint (h)	Replicate	Total RNA yield (µg)	tRNA yield (µg) *
control	0	1	740	8.774
control	0	2	1303.5	1.850
control	0	3	871.6	3.809
control	2	1	1506	3.766
control	2	2	4583.5	4.530
control	2	3	3213.2	8.115
control	24	1	14169	12.897
control	24	2	6445	1.825
control	24	3	4003	7.242
0.5 mM	0	1	775.7	14.157
0.5 mM	0	2	1157	1.445
0.5 mM	0	3	663.5	4.434
0.5 mM	2	1	1025	10.213
0.5 mM	2	2	2486.5	3.645
0.5 mM	2	3	1319.5	5.370
0.5 mM	24	1	6636	15.675
0.5 mM	24	2	5085	5.550
0.5 mM	24	3	4462	2.229
2 mM	0	1	885.1	11.417
2 mM	0	2	1632.5	2.020
2 mM	0	3	832.5	8.071
2 mM	2	1	653.9	8.235
2 mM	2	2	1160.5	2.785
2 mM	2	3	4678.5	8.197
2 mM	24	1	9745.5	13.355
2 mM	24	2	5556.6	4.795
2 mM	24	3	695	5.065

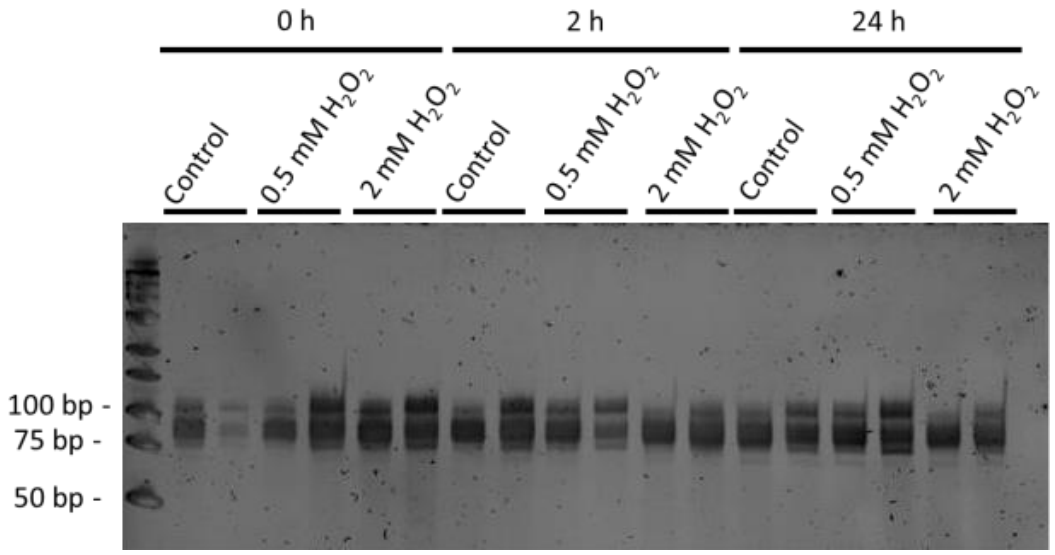

Figure 4.3. Denaturing polyacrylamide gel (10%) electrophoresis analysis of tRNA isolated from control and H_2O_2 treated yeast. 100 ng RNA was loaded and stained with SYBR™ Gold. As size reference, Low Range DNA Ladder (Thermo Scientific™) was used. Each sample is represented with two lanes, as tRNA was isolated with elution buffers containing 750 and 800 mM KCl and checked separately.

4.3. Isolation of ribosomes and rRNA after oxidative stress treatment

To isolate the rRNA yeast, 80S ribosomes were isolated using ultracentrifugation through a sucrose cushion. In both control and treated samples, this step was successful as glass-clear pellets were visible. However, due to handling mistakes during rRNA isolation from the ribosomes, only control sample rRNA was retrieved. Due to time constraints, this experiment was not repeated but the control sample rRNAs were used for downstream MS analyses. Yields of rRNAs from this experiment were estimated after NanoDrop measurements, and they were 47 µg, 40 µg and 78 µg (for each of the replicate cultures). Quality check on 1% agarose gel also showed that isolated rRNA molecules are of good quality with negligible degradation detected as smearing (Fig. 4.4). The two bands visible in the figure are corresponding to 18S (1800 nucleotides long) and 25S (3396 nucleotides long) (Woolford & Baserga, 2013). Lower signal of the bands in rRNA replicate 3 is due to wrong initial estimate of the concentration and yield by NanoDrop, resulting in loading below 200 ng of this samples instead of 500 ng.

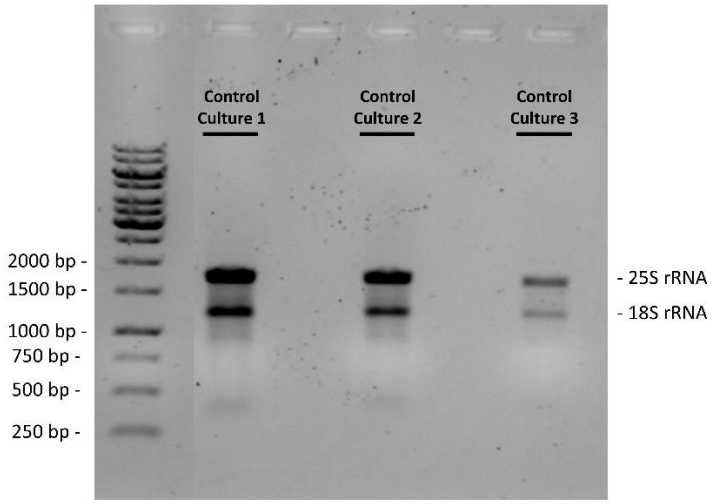

Figure 4.4. Agarose gel electrophoresis of rRNA isolated from purified yeast ribosomes. 500 ng RNA was loaded and as size reference 1 kb DNA Ladder, (Thermo Scientific™) was used. As the treatments were done in triplicate, all 3 replicates from untreated cells are shown in the figure.

Purification of ribosomal proteins was also done during trial runs with control yeast cultures, in order to check for known signals of ribosomal proteins on SDS-PAGE. Result is shown in Fig. 4.5 and the bands present on the gel are corresponding to previously known signals of yeast ribosomal-proteins (Ishiguro, 1976; Planta & Mager, 1998).

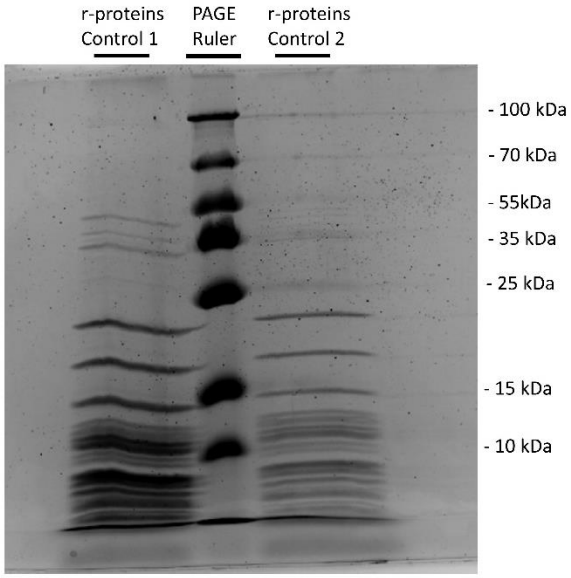

Figure 4.5. Ribosomal proteins purified from yeast 80S ribosomes, run on SDS-PAGE (10% PA separation gel and 4% PA stacking gel).

4.4. Dynamics of tRNA modifications during growth and stress

tRNA modifications present in yeast samples treated with hydrogen peroxide were identified using UPLC/MS analysis, with 50 ribonucleoside standards (list including full names, abbreviations and masses available in Table 7, Materials and Methods section) as references for correct identification of retention times and mass spectra. As the number of available standards was limited, only limited number of known modifications were identified with certainty here. From the available standards, 29 ribonucleosides were identified: 4 canonicals (A, C, G, U) and 25 modified ribonucleosides (ac^4C, ac^6A, A_m, C_m, cnm^5U, G_m, I, I_m, m^1A, m^1G, m^1I, $m^{2,2}G$, m^2G, m^3C, m^4C, m^5C, m^5U, m^6A, m^7G, mcm^5s^2U, mcm^5U, ms^2m^6A, ncm^5U, U_m, Ψ). All identified modifications are known to be present in eukaryotic tRNAs, several of them conserved and present in all 3 domains of life (Bacteria, Archaea, Eukaryota) and in several RNA species besides tRNA (MODOMICS database).

Quantification of the present modifications was done using peak intensity results for all identified modifications. Peak intensities were normalized to a canonical to reflect the variances in the amount of input RNA. For tRNA samples, cytidine ion with *m/z* = 112 was chosen, as peak intensity variation within cytidine ions seemed the least. In order to check how levels of modifications change during time in physiological conditions, the abundance of modifications was compared between investigated time-points in control samples (Fig. 4.6). Only small differences in abundance through time are found, indicating that most identified nucleosides did not change during growth (Fig. 4.6). However, for methylated A (m^1A), G (m^1G, m^2G, m^7G) and C (m^5C) there is a fluctuation in abundance during growth of untreated cultures.

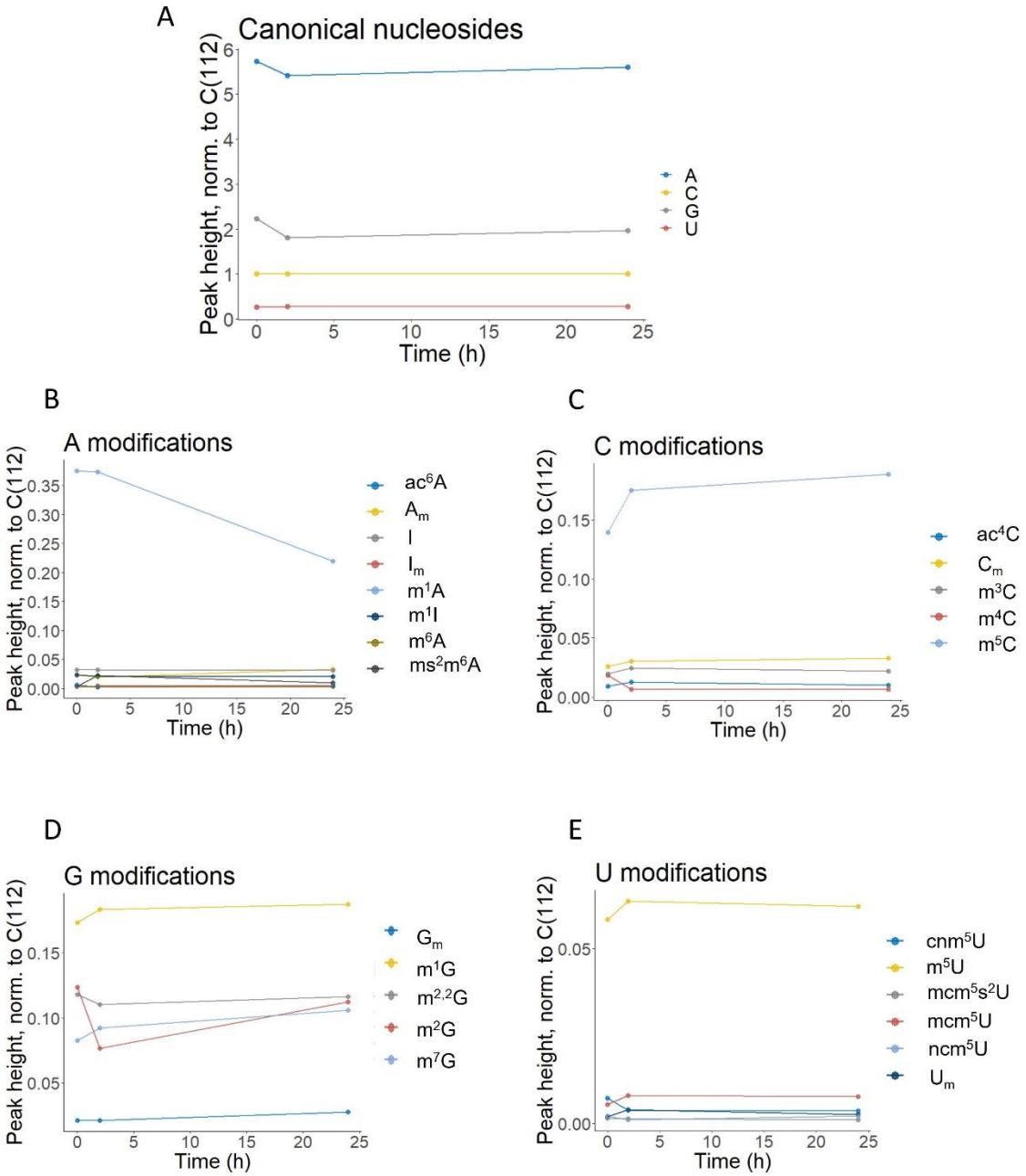

Figure 4.6. Modifications in yeast tRNA from control samples through time. Peak intensities are presented normalized to C (112) canonical ion and taken as a mean of analyzed samples (n=2). Panel A: Results for canonical ribonucleosides. Panel B, C, D, E: results for modifications on A, C, G and U, respectively.

To assess the dynamics of tRNA modifications related to oxidative stress, identified modifications in the two applied treatments (0.5 mM and 2 mM H_2O_2) were compared to the controls. Changes in peak intensities at both time points (2 and 24 hours after elicitation) were calculates as $\log_2$ ($\log_2$ fold change) transformed ratios of peak intensities in the treatment and in the control. Results are presented in Figures 4.7 (change 2 hours after elicitation), 4.8 (change 24 hours after elicitation) and 4.9 (results for both treatments at both tested time points merged for clear visualization).

As the normalization was done to cytidine, no difference in C levels is found in any of the samples (ratio = 1 <=> $\log_2$(ratio) = 0). Positive changes in other canonical ribonucleosides (A, G, U) are found and indicate that the levels of canonical ribonucleosides increase after stress exposure. Most modifications identified here show no difference between treatment and the control, as the $\log_2$ ratio is close to zero and within the variation found for the canonical ribonucleosides (points close to the dashed red line in Fig. 4.7 and 4.8, white blocks in heatmap Fig. 4.10).

Two hours after elicitation (Figure 4.7), strongest decrease is found for ms^2m^6A in both treatments. Modification ms^2m^6A is present in over 8 times lower amount in the 0.5 mM H_2O_2 stressed samples than in the control, and in almost 2 times lower amount in the higher H_2O_2 dosage. In 0.5 mM H_2O_2 treated samples, clear decrease was shown also for mcm^5U, ac^4C and mcm^5s^2U. On the other hand, in 2 mM treated samples there is only ac^4C decrease, and the other two mentioned modifications show a slight increase.

Strongest increase 2 hours after elicitation was found for both treatments in modifications ncm^5U, m^4C, cnm^5U, ac^6A and m^2G. Increase in ncm^5U is the highest and seems to be dose-dependent, as the higher dosage of H_2O_2 treatment showed higher increase. Additionally, in 2 mM H_2O_2 treatment it appears that the presence of m^6A has increased.

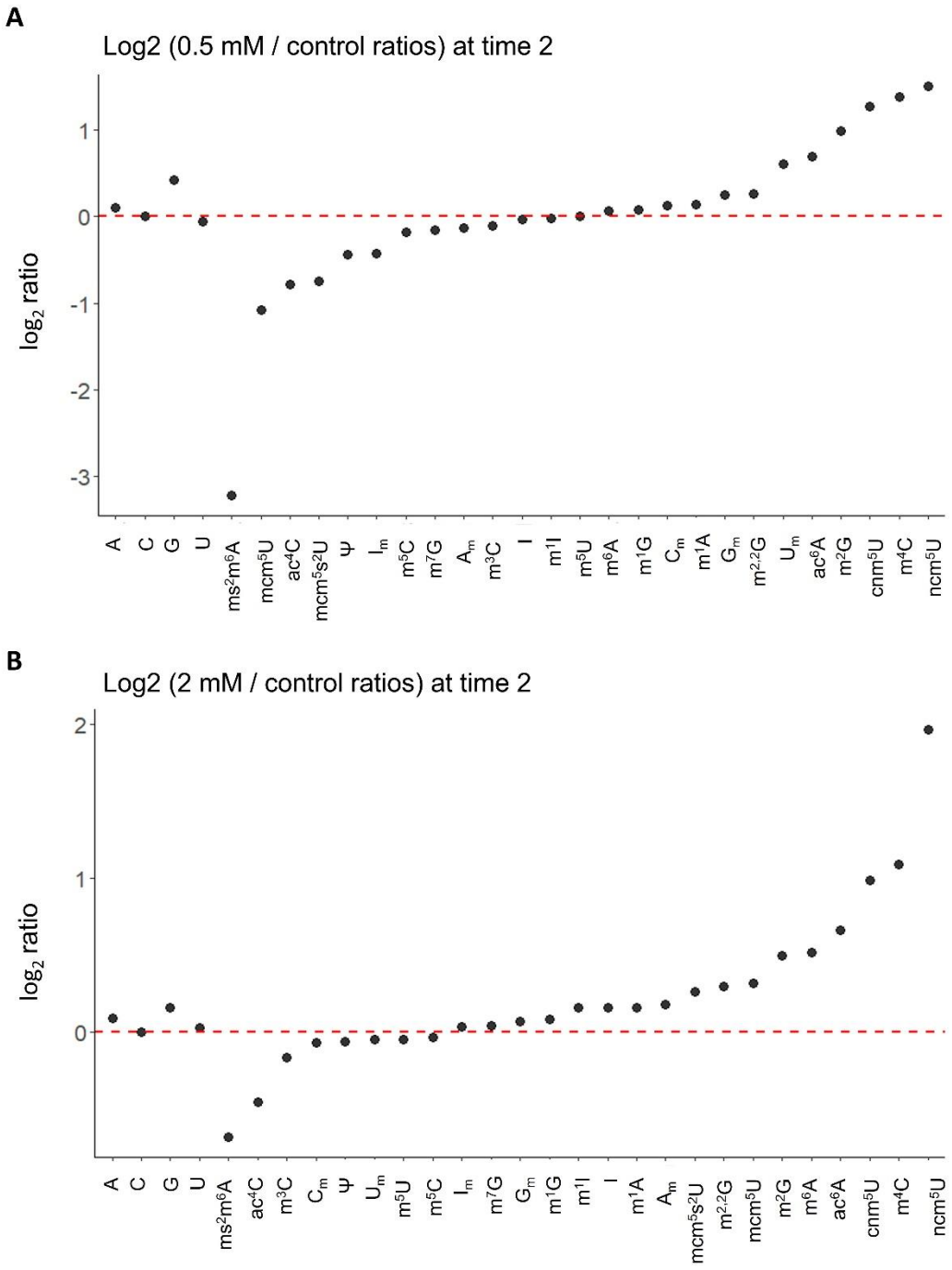

Figure 4.7. Ribonucleoside modifications change in 0.5 (A) and 2 mM treated yeast cultures (B), 2 hours after elicitation. Change is shown for each identified ribonucleoside (including canonicals) as log_2 transformed ratio between normalized intensity of the strongest ion in treated and untreated samples. As the samples were run in duplicate, ratio was calculated from the arithmetic mean. Red dashed line represents log_2 ratio value 0, meaning no change between intensities in treated and untreated samples.

Twenty-four hours after elicitation (Figure 4.8), strongest decrease is found for ac^6A (in 2 mM H_2O_2) and m^4C (in both treatments). Modification m^4C is present in almost 4 times lower amount in the 0.5 mM H_2O_2 stressed samples than in the control, and in around 1.5 times lower amount in the higher H_2O_2 dosage. ac^6A modification level in 0.5 mM H_2O_2 treated cells is not clearly different from the control. In 0.5 mM H_2O_2 treated samples, clear decrease was shown not shown for any other modifications.

Strongest increase 24 hours after elicitation was found for both treatments in modifications ms^2m^6A, cnm^5U, m^1A, m^6A, mcm^5s^2U, U_m and ncm^5U. Comparing the effect sizes in the two different doses, it is clear that dynamics of several modifications are the same: greater increase is shown after 0.5 mM H_2O_2 treatment than after 2 mM for m^1A, ms^2m^6A, cnm^5U, U_m and ncm^5U. Modification m^6A level was clearly increased to the same extent in both treatments. Only modification with higher increase extent in 2 mM H_2O_2 treatment than in 0.5 mM H_2O_2 treatment was mcm^5s^2U. Additionally, in 2 mM H_2O_2 treatment it appears that the presence of $m^{2,2}G$ has increased, even though the increase in 0.5 mM H_2O_2 treated samples was not higher than the variation in the canonicals. Inversely, ac^4C levels are increased in the 0.5 mM H_2O_2 treated samples and in 2 mM H_2O_2 there is no clear difference from the control.

Overall, distinct dynamics of stress-related change is found in several modifications. Assuming that the changes in modifications levels are regulated as part of the oxidative stress response to the treatments, it is shown that modifications which are downregulated 2 hours after elicitation, are also upregulated 24 hours after elicitation, and vice versa (Figure 4.9). Downregulation at 2 hours followed by upregulation at 24 hours is seen for ms^2m^6A, ac^4C and mcm^5s^2U. Reverse is shown for m^4C. It is also evident that in both treatments levels of certain modifications were upregulated in both time points (ac^6A, cnm^5U and ncm^5U). The rest of the identified modifications showed no clear pattern of change within treatments and time points tested.

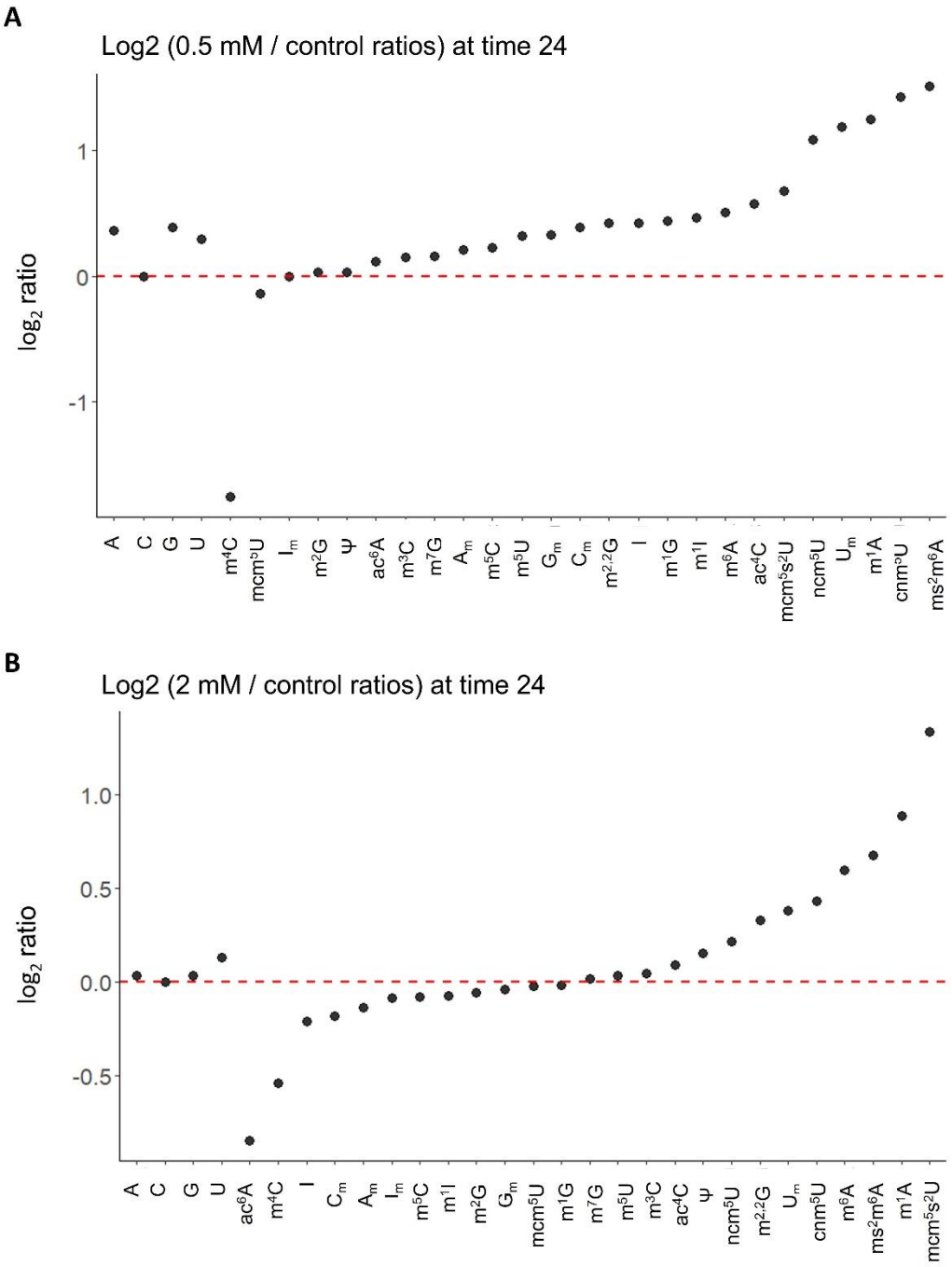

Figure 4.8. Ribonucleoside modifications change in 0.5 mM (A) and 2 mM treated yeast cultures (B), 24 hours after elicitation. Change is shown for each identified ribonucleoside (including canonicals) as log_2 transformed ratio between normalized intensity of the strongest ion in treated and untreated samples. As the samples were run in duplicate, ratio was calculated from the arithmetic mean. Red dashed line represents log_2 ratio value 0, meaning no change between intensities in treated and untreated samples.

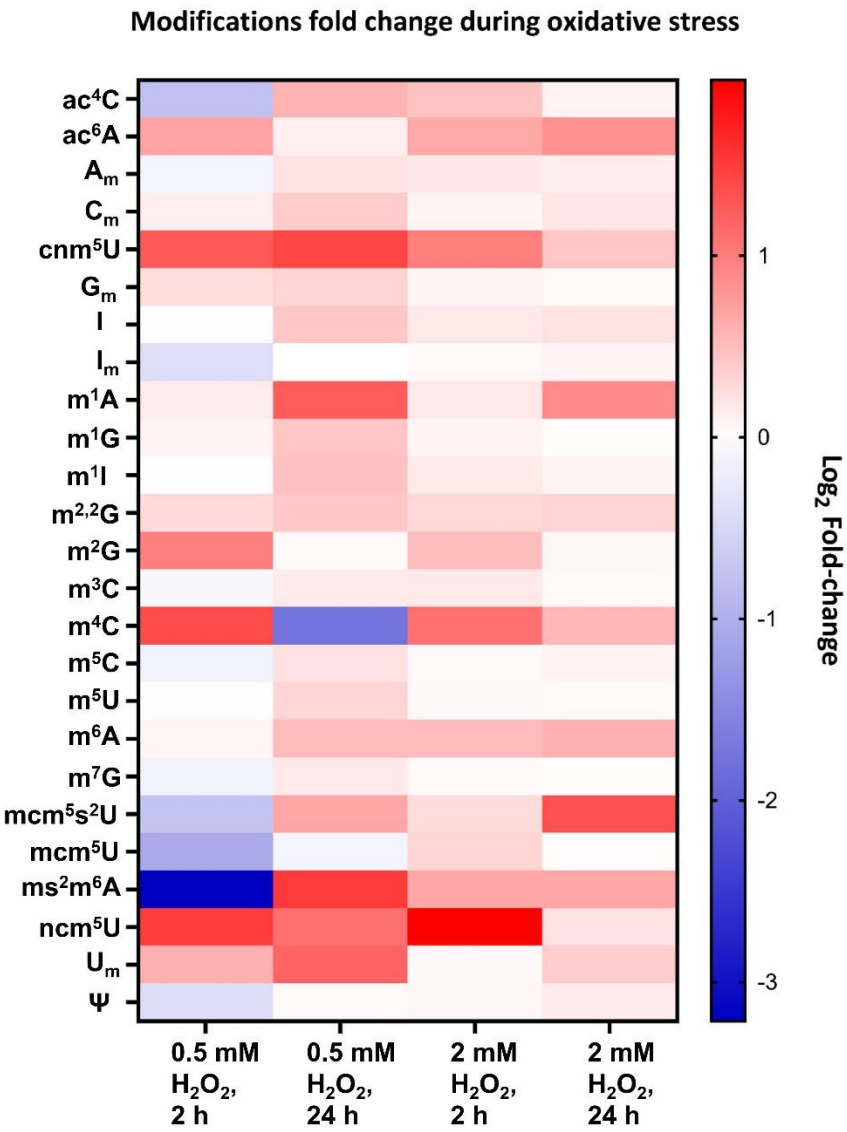

Figure 4.9. Heatmap showing $\log_2$ fold change during oxidative stress for all identified modifications (canonicals excluded). 2 h represents time-point 2 hours after elicitation, and 24 h is 24 hours after elicitation. Results for both H_2O_2 treatments used are shown (0.5 and 2 mM). Heatmap created using GraphPad Prism (version 9.0.0 for Windows).

4.5. Presence and abundance of rRNA modifications

rRNA modifications present in untreated yeast samples were identified using UPLC/MS analysis, with 50 ribonucleoside standards (list including full names, abbreviations and masses available in Table 7, Materials and Methods section) as references for correct identification of retention times and mass spectra. As the number of available standards was limited and intended for tRNA modifications originally, only limited number of known modifications were identified with certainty here. Other modifications known to be present in rRNA molecules were identified as well, given that many of them have unique mass spectra and may be identified manually in the data.

In total, 29 ribonucleosides were identified: 4 canonicals (A, C, G, U) and 25 modified ribonucleosides (m^6A, $m^{6,6}A_m$, ms^2t^6A, ht^6A, t^6A, m^1A, A_m; G_m, OHyW, OHyWy, m^7G, $m^{2,2,7}G$, yW, yW-58, yW-72, yW-86; C_m, m^5C, ac^4C_m, hm^5C; Ψ, m^5U, cm^5U, mcm^5U, m^5D). Identified modifications are known to be present in eukaryotic rRNAs, several of them conserved and present in all 3 domains of life and in several RNA species besides rRNA (MODOMICS database).

Peak intensities for each identified modification were normalized to a canonical to reflect the variances in the amount of input RNA. For rRNA samples, cytidine ion with *m/z* = 244 was chosen, as the signal intensity is within the linear detection range of the instrument. Results are shown as average of the three replicates, with standard deviations calculates. Greatest variation is found in the presence of ncm^5U and A_m, followed by m^5U, OHyWy, G_m, ac^4C_m and hm^5C.

Peak intensities found for adenosine are exceptionally high, in comparison to other canonical nucleosides, indicating enrichment in adenosine in yeast rRNA tested. To check if known sequence is adenosine-rich, ribonucleotide content of ribosomal DNA was estimated using sequences available in *Saccharomyces* Genome Database (www.yeastgenome.org). No enrichment of A was found in rRNA sequences (Table 2). As the samples were isolated from 80S ribosomes, high amount of A may be due to the presence of poly-A tails, typically found in mRNA molecules.

Modifications found here are mostly different methylations of all 4 canonicals, which is expected from previous rRNA modifications research. The abundance of those modifications is low and approximately 100 times lower than the abundance of the canonicals (exception to

that are modifications found on C, where the abundance is 20 times lower than the canonical C).

Modifications typically found in tRNA molecules were found in the tested rRNA samples. Exceptionally high levels of ncm^{5}U were found (Figure 4.10 A), and other well-known tRNA modifications were found to be present in low levels: ht^{6}A, t^{6}A, ms^{2}m^{6}A (Fig. 4.10 B); hypo- and hypermodified wyosine and wybutosine (Fig. 4.10 D).

Table 2. Nucleotide content of rRNA gene sequences. Sequences available at Saccharomyces Genome Database, and content calculated using available web-based GC content calculator (www.sciencebuddies.org/science-fair-projects/references/genomics-g-c-content-calculator).

rRNA gene	Sequence ID	Sequence length (nt)	A (%)	T (%)	G (%)	C (%)
35S rRNA	YNCL0020C RDN37-2	5354	26.58	26.58	27.3	19.54
25S rRNA	YNCL0021C RDN25-2	3396	26.47	25.59	28.45	19.49
18S rRNA	YNCL0025C RDN18-2	1800	26.83	28.33	25.5	19.33
5.8S rRNA	YNCL0014C RDN58-1	158	25.95	27.85	23.42	22.78
5S rRNA	YNCL0031W RDN5-6	121	24.79	23.14	27.27	24.79

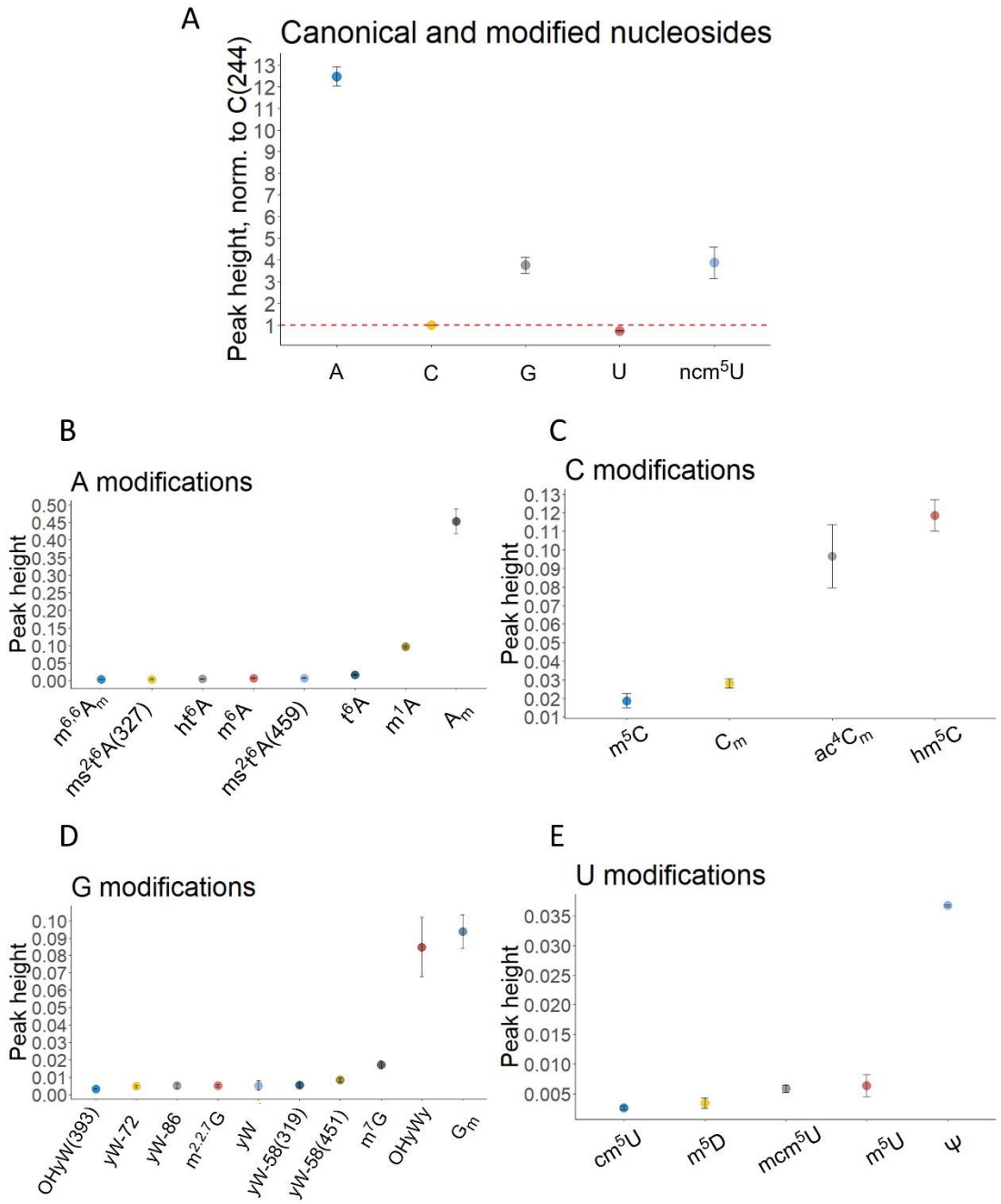

Figure 4.10. Presence and abundance of modifications in yeast rRNA. Peak intensities are presented normalized to C (244) canonical ion and taken as a mean of analyzed samples (n=3). Error bars represent standard deviation. Panel A: Results for canonical ribonucleosides. Panel B, C, D, E: results for modifications on A, C, G and U, respectively. ncm^{5}U is presented together with canonical nucleosides (Panel A) due to scaling.

5. Discussion

5.1. Hydrogen peroxide reduces yeast growth and cell survival

In order to induce oxidative stress that may result in tRNA modification changes, yeast growth was measured in the presence of 0.5 mM and 2 mM H_2O_2 to find the optimal concentration of stressor to avoid lethal dose. The concentrations were chosen to reflect a potentially naturally occurring situation, which might happen during infection (Abegg *et al.* 2010, Briones-Martin-Del-Campo *et al.* 2014). Cell viability was estimated to be 58% and 16% for 0.5 mM and 2 mM H_2O_2, respectively, indicating that a gradient of lethality was applied, after which a bigger or smaller portion of the population of cells survived and recovered from the stress.

Chan *et al.* 2010 have used similar approach to check the oxidative stress-related changes in tRNA modifications, but they reported different results of cell survival than what is shown here (they found 80% survival with 2 mM H_2O_2). Difference between that study and this one may have arisen due to collection time point (here used 2 hours after elicitation, Chan *et al.* 2010 used 1 hour after elicitation) and differences in culturing media and conditions as H_2O_2 in media with heavy metals and anions (Nicoll & Smith, 1955).

In all experiments done here, OD_{600} measures show a difference in survival between control and stress samples 2 hours upon elicitation (Fig. 4.1A, Fig. S1A and S2A). Decrease in OD_{600} in stressed cultures is found, but the effect size is minor in cultures stressed with 0.5 mM H_2O_2 according to the OD_{600} results, indicating no clear effect on yeast growth. OD_{600} is used often in microbiology as estimate for cell concentration and number, where OD_{600} of 1.0 is roughly 3×10^7 cells/mL for yeast cultures. This estimate can vary greatly, especially with stressors in the cell culture which can induce cell death so the absorbance can be influenced. Unviable cells which are not lyzed can skew the cell number estimate, as they contribute to the turbidity measurement. Stress can influence the cell size as well, which may lead to additional discrepancy between OD_{600} and cell count (Turner *et al.* 2012).

Due to that, viable cell counts were done using standard plating of culture dilutions. Dilutions were chosen to be 10^{-4} and 10^{-5} for t_0 and t_1, and 10^{-5} and 10^{-6} for t_2, as the number of cells were most accurately estimated based on previous experiments on non-treated samples. Recommendation in standard microbiological experiments is to use dilutions were the number of colonies on a plate vary between 30 and 300 (Clark, 1965) and here that was taken as a rule.

Viable cell count results showed clearly that survival is lower in both of the treatments than in the control 2 hours after elicitation (Fig. 4.1B, S1B and S2B). However, 24 h after elicitation data shows that cells do recover from treatment, as all cultures show high number of viable cells and no difference between the treatments and the control. As the treatment was done as one dose at elicitation time-point, found recovery and growth hours after the elicitation are expected. Given the unstable nature of H_2O_2 in solutions with heavy metals and anions (Nicoll & Smith, 1955), it is likely that it decomposes through time in the yeast culture, lowering the stress effect and facilitating recovery of the yeast.

5.2. Total and transfer RNA of H_2O_2 stressed yeast isolated

The total RNA from control and treated yeast cells was isolated using hot phenol method. Benefit of using this method is that it is unbiased for all RNA species in the samples, and the resulting high yields. Quality of the total RNA isolated was satisfactory as most samples did not have visible degradation (Fig. 4.2). Challenge of this method was in dissolving the total RNA pellets in distilled water, as the pellets were big and incomplete resuspension could have skewed the concentration and yield estimates.

Total transfer RNA was isolated using anion-exchange chromatography using Nucleobond AX-100 solid-phase cartridge column and using 3 elution buffers with different concentration of KCl (700, 750, and 800 mM KCl buffers). Nucleobond AX-100 is optimized for plasmid DNA isolation, with the column capacity of binding 100 µg DNA. In most yeast total RNA samples precisely 100 µg was loaded onto the columns, despite the exact capacity of binding RNA to this column has not been determined. Yields from tRNA isolation were consistently below 5 µg (lower threshold for running the downstream analyses). As the capacity of the column is not precisely known, it is possible that applied RNA amount was low and material loss high. In addition, such results may be due to handling issues during the recovery of tRNA from the eluted fractions and washing with 80% ethanol steps. Another potential reason for low tRNA yields may be the use of hot phenol method for total RNA isolation. That method is unbiased for all RNA species and small RNA species (such as tRNA) are not preferentially isolated. Thereby, they do make up a proportionally smaller part of the total RNA, in comparison to other methods (TRIzol reagent method, for example). Due to that, multiple samples had to be re-isolated in order to increase the tRNA yield and in final experiment, column was overloaded (130 µg total RNA applied) in attempt to address the issue.

In addition, optimization was done for the elution. During trial isolations and first samples processed it was evident that most tRNA gets eluted immediately in buffer 700, but there is still tRNA even in the highest salt concentration. Due to that, in final experiment samples were eluted with buffers 750 and 800 only. In a small proportion of samples, small rRNA molecules were eluted with 800 mM KCl buffer and the amount of the 5S rRNA contamination was estimated to be 7.5% (quantification of signals on the gel estimated using ImageJ). Due to the signal on the gels being weaker than the tRNA signals and only present in some samples, it was assumed that rRNA contamination would not significantly affect the downstream results.

Considering the knowledge about tRNA-derived fragments (tRFs) from previous research (Thompson & Parker, 2009; Thompson *et al.* 2008; Holcik & Sonenberg, 2005), specific signals of the fragments were expected to be seen on denaturing polyacrylamide gels. Such signals would be visible below the tRNA bands around 40 and 50 bp, as specific bands. However, specific tRF signals were not detected in the samples and the only signals of degradation were nonspecific, visible as smearing (Fig. 4.3). It is possible that tRF signals would be detected when higher amount of tRNA is loaded in the gel, as the proportion of tRFs is potentially several fold smaller than the proportion of full length tRNAs.

Regardless of low yields, when checked on polyacrylamide gels, most tRNAs were of good quality with clearly visible total tRNA cluster between 75 and 100 bp (Fig. 4.3). Several samples from both control and treatments had visible degradation (smearing under the bands visible on gels), but they were used for further analyses due to time constraints.

5.3. Yeast 80S ribosomes and rRNA isolated

As the rRNA isolation from 80S ribosomes was successful in only non-treated samples due to handling mistakes, repeat of this experiment is recommended to obtain rRNA from stressed samples. Due to time constraints, repeated experiment was not done during the scope of this thesis and results of PTM identification here will serve as a reference for the future experiments.

Quality check using urea-PAGE showed the presence of small rRNA species 5S and 5.8S rRNA, as well as signals of tRNAs (found during trial runs, results not shown). As the rRNA was isolated from 80S ribosomes after arresting translation with cycloheximide, it was

expected that tRNAs currently interacting with the ribosomes during translation would be found, as well as mRNAs on the ribosomes. That result was expected, but it is unclear whether downstream analysis is significantly affected. It is possible that modifications present in tRNA only are separated from the analysis of UPLC/MS data, but modifications present in both RNA species are affected so their quantification in rRNA is not precise. As some modifications appear in both rRNAs and tRNAs, completely disregarding "only in tRNA" modifications in the results might hinder the identification of modifications in rRNA.

Isolation of rRNA from 80S ribosomes was chosen here in order to identify rRNA modifications from actively translating ribosomes, instead of total rRNA population of the cells. To avoid potential contamination mRNA and tRNA contamination, other approaches could have been used for rRNA isolation, one example being isolation of rRNA from total RNA using preparative agarose gel extraction. That approach could have been valuable for the analysis of rRNA modifications by mass spectrometry. In addition, separation of rRNA species (25S, 18S, 5.8S and 5S rRNA) would be enabled, facilitating identification of modifications in each rRNA type. As total RNA from control and treatments is still available and may be used for such analyses, that approach might be implemented in future experiments.

5.4. RNA digested to ribonucleosides and analyzed by UPLC/MS

Prior to the UPLC/MS analysis, tRNA and rRNA samples were digested to ribonucleosides enzymatically and purified with the HyperSep HyperCarb Spin tips to obtain mononucleosides. Completeness of the digestion was assessed by checking the peak shift from 260 to 255 nm. As the individual ribonucleosides have lower absorption peaks than RNA (Rodger, 2013), peak shift can be used for this kind of assessment. Additional check should be done at that step to ensure digestion was complete, and that is by running the samples on PAGE, where presence of tRNA and rRNA specific bands would have been the evidence that cleavage was not complete. That way it would be possible to repeat the digestion or estimate which proportion of the samples are digested incompletely. However, due to low amounts of starting RNA material (primarily in tRNA samples), digestion was only checked by 260-255 nm shift estimation here.

As the MS analysis is done within the detection range of *m/z* 100-600, mononucleosides are detected and impurities of lower and higher mass such as ribose fragmentation products

and polynucleotides are not detected. Quantification of the ribonucleosides is based on loaded equal amounts of the digested samples, and to correct for the potential differences in loading amounts, normalization to a canonical is done. Due to all that, small portion of uncleaved RNA in the prepared samples should not hinder the analysis.

In addition, due to low amounts of starting tRNA material, samples from only two experiment replicates were chosen for digestion and further analysis. By re-isolating the tRNA from already available total RNA from treated and non-treated yeast, it would be possible to address the issue of few replicates and repeat the analysis.

5.5. Oxidative stress-related reprogramming of tRNA modificome

tRNA modifications present in yeast samples treated with H_2O_2 were identified using UPLC/MS analysis. Results show that 29 nucleosides were identified from the 50 ribonucleoside standards used as references for identification (Gregorová *et al.* 2020). All identified modifications were according to the expectations, as they are known to be present in eukaryotic tRNAs (MODOMICS database). However, several known eukaryotic tRNA modifications were not identified here, including cm^5U, imG-14, m^1Y, $m^{2,7}G$, m^5s^2U, s^2U and f^5C. Although their presence was not confirmed here, that could be expected because not all modifications are present in all conditions and their abundance combined with ionization propensity causes the signal to fall below the cutoff limit (Gregorová *et al.* 2020).

To identify and quantify ribonucleoside modifications, peak intensity signals from UPLC/MS were used as a measurement of the modification abundance. Peak intensities for each identified modification were normalized to a canonical to reflect the variances in the amount of input RNA. For tRNA samples, cytidine ion with $m/z = 112$ was chosen, as the signal intensity is within the linear detection range of the instrument. Differences within ribonucleosides' ions stem from variation in ionization efficiency (Sarin *et al.* 2018), and that was considered for all ribonucleosides. The strongest ion was chosen for all ribonucleosides and used to compare abundance in stressed versus control samples. Easier visualization and interpretation of the results was enabled due to the comparison of only one ion for each ribonucleoside.

Modification levels are dynamic, reflecting both the growth phase of the cells as well as environmental conditions. So minor fluctuation in modifications during yeast culture growth

shown here for all identified ribonucleosides (Fig. 4.6) is in accordance with previous research (Heiss *et al.* 2017). However, strongest fluctuations are observed for m^1A, m^2G and m^5C. It is possible that Dimroth rearrangement hindered the identification and precise quantification of m^1A, as it is known to rearrange into m^6A in alkaline conditions as a function of pH (Macon & Wolfenden, 1968). Identifying signals from all ribonucleosides was manually curated, finding signals of isomers by comparing the 4 standard mixes and complex mix orders in which isomers elute. Order of their appearance in standard mixes was then taken as a rule of thumb for identifying them in the samples as well (Gregorová *et al.* 2020).

Increase in canonical ribonucleosides (A, G, U) was found, indicating higher levels after stress exposure. From this result, it may be assumed that modification levels have decreased after stress exposure. However, such a direct conclusion cannot be made, as the identified modifications show both increased and decreased levels (Fig, 4.7, 4.8, 4.9). Due to few replicates tested here, the variation in modification abundance in treated and non-treated samples could not be tested and statistical significance was not established. Most identified modifications showed no change in abundance, which is to be verified with additional replicates. However, distinct dynamics of stress-related change was found for several modifications, which is consistent with previous research in stress-related modificome reprogramming, in numerous unicellular organisms (Chan *et al.* 2010, Chan *et al.* 2012, Fernández-Vázquez *et al.* 2013, Puri *et al.* 2014, Sun *et al.* 2018, Leiva *et al.* 2020).

Downregulation at 2 hours was seen for ms^2m^6A, ac^4C, mcm^5U and mcm^5s^2U. Reverse is shown for ncm^5U, cnm^5U, ac^6A, m^2G and m^4C. This result is consistent with previous research for mcm^5s^2U modification, as it was known to be downregulated after exposure (Chan *et al.* 2010, 1 hour after elicitation tested in their study). A homeostasis model of the modification dynamics associated with oxidative stress response was proposed in previous research (Chan *et al.* 2012), and the key feature of the model is cooperativity of modifications. The stress-induced change in a certain modification may be a response to a change occurring with another modification. As other modifications on U (ncm^5U and cnm^5U) were shown to be upregulated, it can be assumed that during stress those are present instead of mcm^5s^2U and mcm^5U, in consistence with the proposed model. Furthermore, mcm^5s^2U formation is known to be dependent on two enzymatic pathways, ELP and URM1 (Noma *et al.* 2009, Leidel *et al.* 2009, Dauden *et al.* 2019, Pabis *et al.* 2020), so decrease in this modification during stress may point to further research in those pathways.

Furthermore, other modifications were found to be major features of H_2O_2 stress response before, notably m^5C, $m^{2,2}G$, C_m and t^6A (Chan *et al.* 2010). That appears not be the case here, revealing additional modifications that may play a role in stress related modificome reprogramming.

Previous studies have identified the roles of the modifications using cell survival as phenotype proxy for sensitivity of the yeast and various yeast mutants to oxidative stress. They have not identified modifications after several generation times (e.g. 24 hours, as it was done here). It was expected that recovery of culture growth after 24 hours (Fig. 4.1) may be accompanied with modification level return to the level present in control cultures. As the cultures are in stationary phase 24 hours after elicitation (volume of the cultures was constant, see section 3.2), that expectation may not be true due to various physiological changes found in "over-grown" cultures (Nyström, 2004). Comparing modification changes near elicitation and well after elicitation (2 hours and 24 hours after), has yielded an additional level of modificome reprogramming understanding. Certain modifications were up- and down-regulated after 24 hours, contrary to the "return to level in control cultures" expectation (Fig. 4.9). Downregulation at 2 hours followed by upregulation at 24 hours was seen for ms^2m^6A, ac^4C and mcm^5s^2U. Reverse was shown for m^4C. It was also evident that in both treatments levels of certain modifications were upregulated in both time points (ac^6A, cnm^5U and ncm^5U).

Downregulation of ms^2m^6A during oxidative stress may be related to mitochondrial stress response via activation of apoptosis (Nawrot *et al.* 2011), as it is a known to be present in mitochondrial tRNA. A consequence of ms^2m^6A downregulation may be destabilization of tRNA structure, as that modification is known to be stabilizing base stacking interactions in single-stranded domains of tRNA and have destabilizing effects in RNA hairpins (Kierzek & Kierzek, 2003). Confirming and further analyzing the oxidative stress consequences on this modification by identifying modifications in mitochondria and during stress-related apoptosis would be beneficial. Further structural analysis of tRNA destabilization in the presence of ms^2m^6A would also confirm the function of this modification.

To study the consequences of stress related changes on translation and elucidate the roles of modifications, it would be of importance to know the positions on tRNA where identified modifications are located. Modifications found to be affected by oxidative stress here are most frequently located on the wobble position 34 (mcm^5U, ac^4C, ncm^5U, cnm^5U, U_m) and anticodon loop position 37 (m^2G). As they are known to be commonly modified positions, it is

expected that changes in their modification levels could affect the tRNA function in translation. Modifications known to be present in other domains of tRNA can also be expected to play a role as change in their abundance may interfere with tRNA structure, as exemplified by ms^2m^6A.

Previous research has pointed towards selective translation as a consequence of tRNA modifications reprogramming during stress (Chan *et al.* 2012, Rezgui *et al.* 2013, Zinshteyn & Gilbert, 2013, Nedialkova & Leidel, 2015). In Chan *et al.* 2012, increase in m^5C at wobble position of a Leu tRNA was shown to cause selective translation of mRNAs enriched in Leu. Although m^5C was not observed here, similar outcomes of modification up- and down-regulation can be expected from results presented here.

Disadvantage of this research is that the change in modifications levels is not clearly identified to arise from modifications being added and erased, or from changes in tRNA presence itself. Different approaches may be used in the future to confirm the results presented here and provide further insight into the modificome dynamics during stress response.

Cleavage of tRNA molecules into tRNA-derived fragments (tRFs) during stress response should be taken into account in future research, because it has been shown in numerous studies on bacteria, yeast and mammalian cells, and it has even been proposed that tRFs are involved in stress-response regulation (Huh *et al.* 2021; Thompson & Parker, 2009; Thompson *et al.* 2008; Holcik & Sonenberg, 2005). Although it was argued that abundance of full-length tRNAs is high and tRNA pool is not significantly depleted when degradation happens, it is possible that those differences influence the tRNA modificome identification and significant depletion of Tyr tRNA is found recently (Huh *et al.* 2021). Also, cleavage is found in unstressed cells in low but detectable amounts (Thompson *et al.* 2008) so taking it in account in future experiments would be reasonable and would benefit further research in modificome dynamics. Fragmentation of rRNA has been shown by the same authors, and that should be addressed in future research as well. Fragmentation of tRNA molecules is notable during late stages of growth, namely stationary phase (Thompson *et al.* 2008), which implies that changes in modificome may be affected by the fragmentation levels in this study as well, especially in t_2, 24 hours after elicitation.

Established methods for identification of PTMs are various and include several versions of mass spectrometry, primer extension essays, antibody pulldowns. Considering all gathered knowledge on modifications presence and abundance, more recent approaches include pairing

with high-throughput sequencing. In Vandivier *et al.* 2018, a new bioinformatics approach was introduced for annotation of modified ribonucleosides based on mismatches patterns. More recently, Zhang *et al.* (2020) developed a new sequencing method that can also identify modified nucleosides. It is based on direct RNA sequencing (no cDNA steps involved) using 2-dimensional mass-retention time hydrophobic end-labeling and MS-based sequencing. It would be of interest to use their approach for further research in PTMs and their changes upon stress.

In order to understand if the changes in modification patterns are due to a change in tRNA presence/abundance itself or if it is because of modification pattern genuine change, it would be necessary to estimate tRNA abundance using quantitative methods like Northern blot and tRNA sequencing. Recently a method has been developed for observation of modification dynamics in existing and newly synthesized RNAs during growth (Heiss *et al.* 2017). NAIL-MS (nucleic acid isotope labeling coupled mass spectrometry) is a method based on pulse-chase labeling approaches, which allows for modificome identification using optimized MS protocols with efficient run times. Coupling isotope labeling with mass spectrometry and novel tRNA-Seq methods would be the way to extensively characterize the dynamics of tRNAs and their modifications (Shigematsu *et al.* 2017, Zhang *et al.* 2020, Behrens *et al.* 2021, Shi *et al.* 2021), providing insights into the stress-related tRNA and tRNA fragments level in the cells alongside modificome. Using tandem mass spectrometry, it would be possible to further check the signals of the modified ribonucleosides and potentially identify novel modifications present in RNA or signals of chemical changes to the modifications known to be present in the samples (Jora *et al.* 2021).

5.6. rRNA modifications landscape

rRNA modifications present in untreated yeast samples were identified using UPLC/MS analysis, with 50 ribonucleoside standards (list including full names, abbreviations and masses available in Table 7, Materials and Methods section). As the rRNA was isolated from 80S ribosomes, all rRNA types were analyzed simultaneously (25S, 18S, 5.8S and 5S rRNA).

In total, 29 ribonucleosides were identified: 4 canonicals (A, C, G, U) and 25 modified ribonucleosides (see section 4.5). Identified modifications were expected as they are known to

be present in eukaryotic RNAs, several of them conserved and present in all 3 domains of life and in several RNA species besides rRNA (MODOMICS database).

Methylations of all 4 canonicals were found here (Fig. 4.10), which is expected from previous rRNA modifications research (Sharma & Lafontaine, 2015). rRNA is known to be modified at approximately 2% (Yang *et al.* 2016), so the low abundance found here is consistent with that. Modifications were found here to be approximately 100 times lower in abundance than the abundance of the canonicals, and the exception to that are modifications found on C, where the abundance is only 20 times lower than the canonical C. As methylated C is known to be present in several positions on rRNA (Li *et al.* 2017, Edelheit *et al.* 2013, Squires *et al.* 2012), this is not a surprising result.

As there were 3 replicates available for the rRNA of control yeast cultures, the results also showed that there is variation in the abundance of certain modifications (ncm^5U, A_m, m^5U, OHyWy, G_m, ac^4C_m and hm^5C, Fig. 4.10). rRNA is not known to be heavily modified (Yang *et al.* 2016), so the high abundance of canonicals found here (Fig. 4.10) was not surprising. However, exceptionally high abundance of A was not expected and as there is no sequence enrichment of A (Table 2), it was clear that high amounts of A indicate the presence of poly-A tails. Poly-A tails are found in mRNAs, so it is likely that mRNAs associated with the isolated ribosomes were analyzed as well.

Modifications typically found in tRNA molecules were also found in the tested rRNA samples (ncm^5U, ht^6A, t^6A, ms^2m^6A, hypo- and hypermodified wyosine and wybutosine, Fig. 4.10). Confirming their presence in rRNA would be of interest, although isolation of rRNA from ribosomes seems to be hindering the analysis, as the presence of both mRNA and tRNA is evident. Separating RNA isolated from 80S ribosomes on agarose gel and isolating only rRNA from the gel, would overcome this issue. At the same time, rRNA modifications from actively translating ribosomes only would be identified.

Available ribonucleoside standards used here were previously optimized for tRNA modifications analysis (Gregorová *et al.* 2020). Therefore, it is possible that standards were not sufficiently informative and detection of a wider range of rRNA modifications was hindered. This issue may be solved in future experiments by acquiring more modified nucleosides specific for the rRNA in the standards. Additionally, analyzing rRNA types separately would enable getting a deeper understanding of which modifications are present and where they are positioned. Using tandem mass spectrometry, it would be possible to confirm the results and

potentially identify the signals of novel modifications present in rRNA, such as ncm^{5}U signal found here.

5.7. Outlook and future developments

Due to all previously mentioned challenges, future research is proposed to confirm the results. Firstly, additional stress experiments should be done in order to isolate ribosomes and rRNA from not only control, but also treated yeast cultures. Other approaches could be used for rRNA isolation than isolation from ribosomes, one example being isolation of rRNA from total RNA using preparative agarose gel extraction. Implementation of that approach would be possible immediately, as total RNA from all conditions and time-point is still available and may be used for such analyses.

Secondly, to confirm if the changes in modification levels are due changes in tRNA abundance or due to honest signal of modifications being added and erased, tRNA sequencing approach should be used in the future.

Finally, to elucidate the role of tRNA and rRNA modifications during translation future experiments using a cell-free translation system (cell-free protein synthesis system CFPS) will be done. CFPS is a flexible tool for studying molecular processes during transcription and translation, as it is system derived from crude cell extract including all parts of the molecular machineries and cofactors. By adding the purified tRNAs and ribosomes from stress conditions, it will be possible to check heterologous protein production efficiency in the presence of different modifications. As it has been hypothesized that ribosomes are differentially modified and may be specialized, it would be of interest to see how translation is affected by stress-related modifications present in the translation machinery.

To assess the translation efficiency and kinetics of the cell-free translation reactions, two types of fluorescence reporter proteins will be used: GFP (green fluorescent protein) variants which can be visualized during the production and thereby shows the dynamics of the process, and firefly luciferase which is visualized by the addition of luciferin (substrate for luciferase) at the endpoint of the translation experiment. It is expected that the modifications located in the anticodon loop have the most influence on translation efficiency, but influence of other modifications cannot be ruled out (for example modifications impacting the aminoacylation rate or stabilizing the structure).

Another approach which could prove useful in deciphering dynamic modificome roles is based on the *in vitro* transcribed (IVT) tRNAs. IVT tRNAs were shown to be active in translation in a cell-free protein synthesis system (Hibi *et al.* 2020), so impact of specific modifications on translation efficiency could be tested by selectively adding tRNAs with certain modifications present. Selective addition of modification to IVT tRNAs can be done by expressing and purifying known modification enzymes, and aminoacylation of the tRNAs (Hibi *et al.* 2020) can be done to ensure activity in CFPS reactions.

This thesis work lays the foundation to study the evolutionary conserved function of PTM changes during stress as modulators of translation and is likely of great importance in the field of heterologous protein production area of biotechnology.

6. Conclusions

Using UPLC/MS analysis, 29 modifications were identified in tRNA from control and H_2O_2 treated yeast. Most identified modifications showed no change in abundance in treatments, which is to be verified with additional replicates. However, distinct dynamics of stress-related change was found for several modifications, revealing additional modifications that may play a role in stress related modificome reprogramming to the previously known signature modifications of oxidative stress.

It was expected that recovery of culture growth after 24 hours may be accompanied with modification level recovery. However, that was not demonstrated here as downregulation at 2 hours followed by upregulation at 24 hours was seen for ms^2m^6A, ac^4C and mcm^5s^2U, and the reverse was shown for m^4C. Upregulation in both time points was also shown here (ac^6A, cnm^5U and ncm^5U). These results confirm a complex and dynamic control of tRNA modifications in cellular survival responses.

Modifications found to be affected by oxidative stress here are most frequently located on the wobble position 34 and anticodon loop position 37, so it is expected that changes in their modification levels could affect the tRNA function in translation, making them a specific target for future research.

In addition to tRNA modifications, modifications in rRNA from control yeast cultures were identified. Methylations of all 4 canonicals were found here, which was expected from previous research. However, further analysis will be needed to confirm the identified modifications, due to the potential mRNA and tRNA contamination. Acquiring more modified nucleosides specific for the rRNA to use as standards in the analysis, analyzing rRNA types separately and using tandem mass spectrometry would enable getting a deeper understanding of which modifications are present and where they are positioned. Finally, it would enable reliable identification of the signals of novel modifications present in rRNA, such as the ncm^5U signal found here which needs to be confirmed.

In conclusion, this thesis work lays the foundation to study the evolutionary conserved function of PTM changes during stress as modulators of translation, using the methodological approaches discussed in-depth here, firstly to confirm the intriguing results found here.

7. Supplement

7.1. Code used for data visualization in R

```
# Libraries needed
library(tidyr)
library(ggplot2)
library(readxl)
library(plyr)
library(ggsci)

# Data path setting
datapath <- "D:/MASTER/YEAR2/master_thesis/growth_curves"


### Growth curves of control and treated yeast ###
##################################################

# Data import from Excel
# OD(600) measurements
od600repl1 <- read_excel(paste0(datapath, "/Growth_curve_exp_week2.xlsx"), sheet =
"replicate1", .name_repair = "minimal")

# Calculate average, standard error of mean, standard deviation
od600repl1.wide <- ddply(od600repl1, c("Sample", "Time.point"), summarise, mean =
mean(OD), sd = sd(OD), sem = sd/sqrt(3))

# Rename samples
od600repl1.wide$name <- "mM"
od600repl1.wide  <- od600repl1.wide %>% unite("Sample", c("Sample", "name"), sep= "
", remove=TRUE)

# Plot mean values through time
od600repl1.base.plot    <-    ggplot(od600repl1.wide,    aes(x=Time.point,    y=mean,
color=Sample))

od600repl1.growth.plot <- od600repl1.base.plot +
  geom_point(size=3, alpha=0.8) + # add points as the plotted observations
 geom_errorbar(aes(ymin=mean-sd,     ymax=mean+sd),     width=.09,     color="black",
alpha=0.8)+ # add error bars
  geom_line(size=1, alpha=0.8) + #add line to connect points
  labs(title = "Yeast growth curve - replicate 1") + # add title
  theme_classic() +
  scale_y_continuous(name="OD600") +
  scale_x_continuous(name="Time (hours)") + # add labels to the x and y axes, both
continuous
  scale_color_jco() +
  theme(text = element_text(size = 20)) # adjust size of letters

# Show and save the result
print(od600repl1.growth.plot)

# All other curves were produced in the same way, for all 3 replicates, and both
OD(600) and CFU/mL measurements

# Growth curve close-up to 2 hours after elicitation:
# Limit the x and y axis by using next lines:
# xlim(-3.5, 2.5) +
# ylim(0, 2) +
```

```
### tRNA modifications in controls across time ###
##################################################

# Data import from Excel
# Canonicals and modifications were plotted separately

canonicals   <-   read_excel(paste0(datapath,   "/tRNA_control.xlsx"),   sheet   =
"canonicals", .name_repair = "minimal")
Amodif  <-  read_excel(paste0(datapath,  "/tRNA_control.xlsx"),  sheet  =  "Amodif",
.name_repair = "minimal")
Gmodif  <-  read_excel(paste0(datapath,  "/tRNA_control.xlsx"),  sheet  =  "Gmodif",
.name_repair = "minimal")
Cmodif  <-  read_excel(paste0(datapath,  "/tRNA_control.xlsx"),  sheet  =  "Cmodif",
.name_repair = "minimal")
Umodif  <-  read_excel(paste0(datapath,  "/tRNA_control.xlsx"),  sheet  =  "Umodif",
.name_repair = "minimal")

# Example plotting for canonicals data:

# Plot canonicals the observation through time
canonicals.base.plot <- ggplot(canonicals, aes(y=measure, x=Time.point, color=ID))
canonicals.plot <- canonicals.base.plot +
  geom_point(size=3, alpha=0.8) + # add points as the plotted observations
  geom_line(size=1, alpha=0.8) + # add line to connect the points
  labs(title = "Canonical nucleosides") + # add title
  theme_classic() +
  scale_y_continuous(name = "Peak height, norm. to C(112)", breaks = seq(0, 13, by =
1)) +
  scale_x_continuous(name = "Time (h)") + # add labels to the x and y axes, both
continuous
  scale_color_jco() +
  theme(text = element_text(size = 30)) # adjust the size of letters

# Show and save the result
print(canonicals.plot)


### tRNA modifications change ###################################
### in treatments 2 and 24 hours after stress elicitation ###
#############################################################

# Data import from Excel
# log2 of ratio 0.5mM / control, at 2 hours after elicitation
data  <-  read_excel(paste0(datapath,  "/for-plots.xlsx"),  sheet  =  "0.5mM_ratio",
.name_repair = "minimal")

# Lock in the modification names as factor levels
# in order of appearance in the data file
data$ID <- factor(data$ID, levels = data$ID)

# Example plotting only for change after 0.5 mM hydrogen peroxide treatment,
# 2 hours after elicitation

# Plot the log2 changes
figure <- ggplot(data, aes(x=ID, y= time2_0.5mM_ratio)) +
  geom_point(size=3, alpha=0.8) + # add points as the plotted observations
  labs(title = "log2 (0.5mM / control ratios) at time 2") + # add title
  theme_classic() +
  ylab("log2 ratio") + #add y axis label
  scale_color_jco() +
  theme(axis.text.x = element_text(angle = 90, vjust = 0.5, hjust=1)) + # adjust the
angle of the x axis tick labels
  geom_hline(yintercept=0, linetype="dashed", color = "red", size=1) + # add a line
of zero change at log2 = 0 as a reference
  theme(text = element_text(size = 20)) # adjust the text size

# Show and save the result
print(figure)
```

```
### rRNA modifications presence in controls ###
################################################

# Data import from Excel
# Canonicals and modifications were plotted separately

canonicals <- read_excel(paste0(datapath, "/rRNA.xlsx"), sheet = "canonicals",
.name_repair = "minimal")
Amodif <- read_excel(paste0(datapath, "/rRNA.xlsx"), sheet = "Amodif", .name_repair
= "minimal")
Gmodif <- read_excel(paste0(datapath, "/rRNA.xlsx"), sheet = "Gmodif", .name_repair
= "minimal")
Cmodif <- read_excel(paste0(datapath, "/rRNA.xlsx"), sheet = "Cmodif", .name_repair
= "minimal")
Umodif <- read_excel(paste0(datapath, "/rRNA.xlsx"), sheet = "Umodif", .name_repair
= "minimal")

# Example plotting only for canonicals and all modifications were done the same way

# Lock in the modification names as factor levels
# in order of appearance in the data file
canonicals$ID <- factor(canonicals$ID, levels = canonicals$ID)

# Plot the normalized peak heights (intensities), normalized to C(244)

canonicals.base.plot <- ggplot(canonicals, aes(x=ID, y=`C244-mean`, color=ID))
canonicals.plot <- canonicals.base.plot +
  geom_point(size=5, alpha=0.8) + # add points as the plotted observations
  geom_errorbar(aes(ymin = `C244-mean`-`C244-stdev`, ymax = `C244-mean`+`C244-
stdev`), width = .09, color = "black", alpha = 0.8) + # add error bars
  labs(title = "Canonical and modified nucleosides") + # add title
  theme_classic() +
  scale_y_continuous(name="Peak height, norm. to C(244)", breaks = seq(0, 13, by =
1)) + # add y axis label and adjust the ticks on y axis frequency
  geom_hline(yintercept=1, linetype="dashed", color = "red", size=1) + # add a line
at normalized intensity 1 as a reference, only for canonicals
  scale_color_jco()+
  theme(legend.position = "none") + # remove the redundant legend
  theme(text = element_text(size = 30)) # adjust the text size

# Show and save the result
print(canonicals.plot)
```

7.2. Hydrogen peroxide impact on yeast growth and cell survival

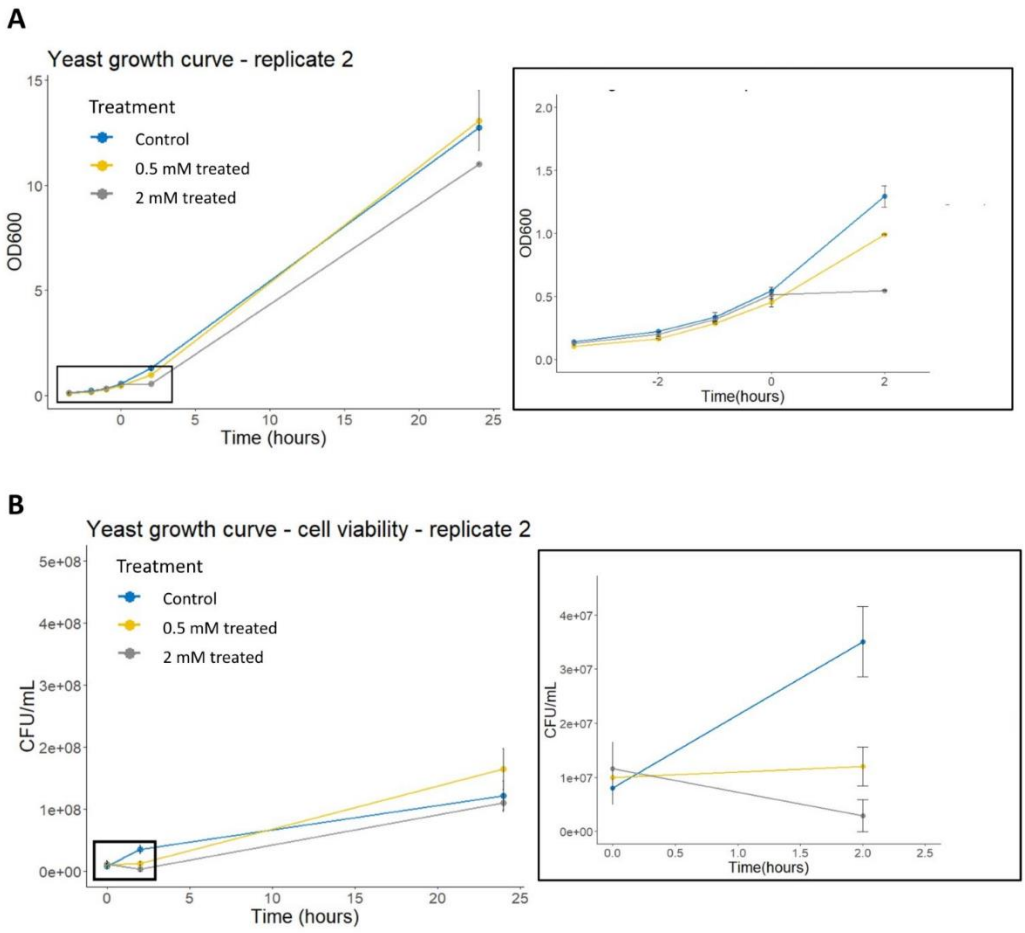

Figure S1. Yeast growth during oxidative stress, biological replicate 2. Panel A: OD_{600} measurements are plotted against time, on the left throughout the full experiment and on the right as a close-up for better visualization of time-points at elicitation and 2 hours after elicitation. Panel B: CFU/mL measurements are plotted against time on the left throughout the full experiment and on the right as a close-up for better visualization of time-points at elicitation and 2 hours after elicitation. Time is in hours, where 0 is the elicitation point, 2 is the stress point and 24 is the recovery (final) point. OD_{600} was measured hourly from 0.2 and those measurements are indicated with negative values of time. Dots represent mean of experiment duplicates and error bars represent the standard deviation.

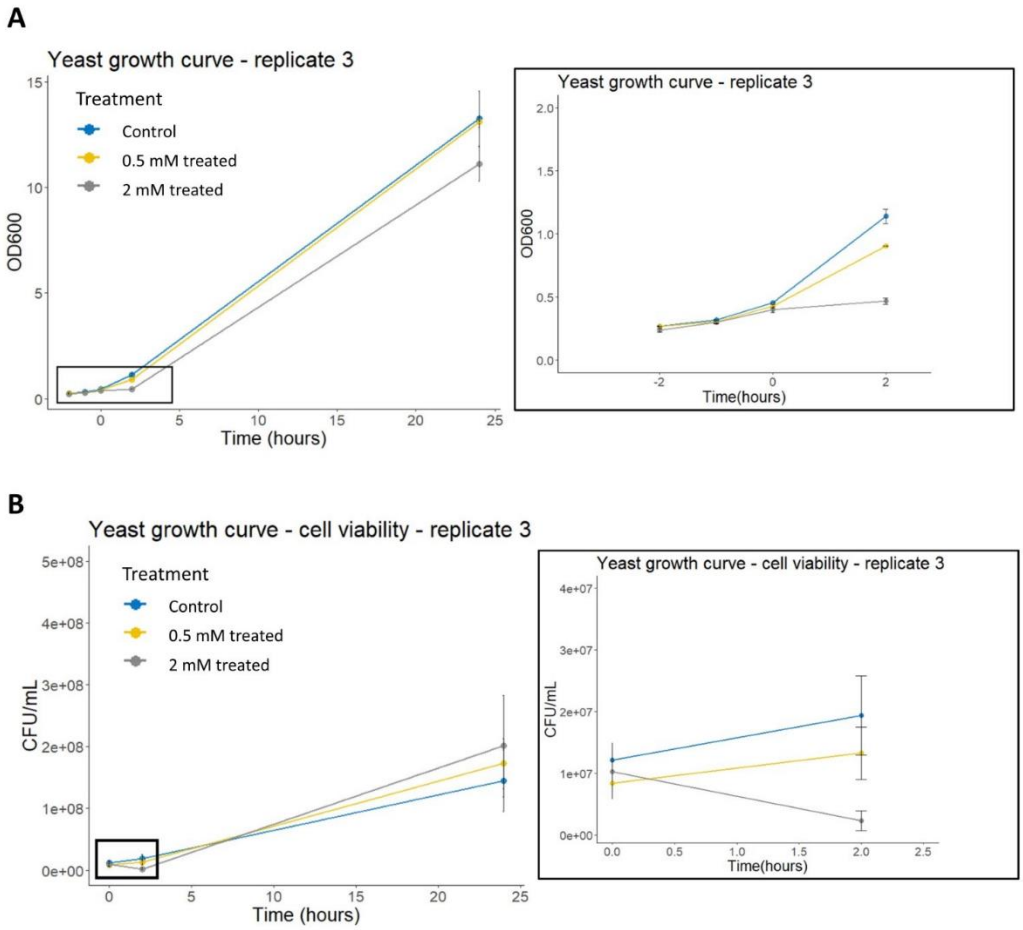

Figure S2. Yeast growth during oxidative stress, biological replicate 3. Panel A: OD_{600} measurements are plotted against time, on the left throughout the full experiment and on the right as a close-up for better visualization of time-points at elicitation and 2 hours after elicitation. Panel B: CFU/mL measurements are plotted against time on the left throughout the full experiment and on the right as a close-up for better visualization of time-points at elicitation and 2 hours after elicitation. Time is in hours, where 0 is the elicitation point, 2 is the stress point and 24 is the recovery (final) point. OD_{600} was measured hourly from 0.2 and those measurements are indicated with negative values of time. Dots represent mean of experiment duplicates and error bars represent the standard deviation.

7.3. Analysis of total and transfer RNA isolated from peroxide stressed yeast cultures

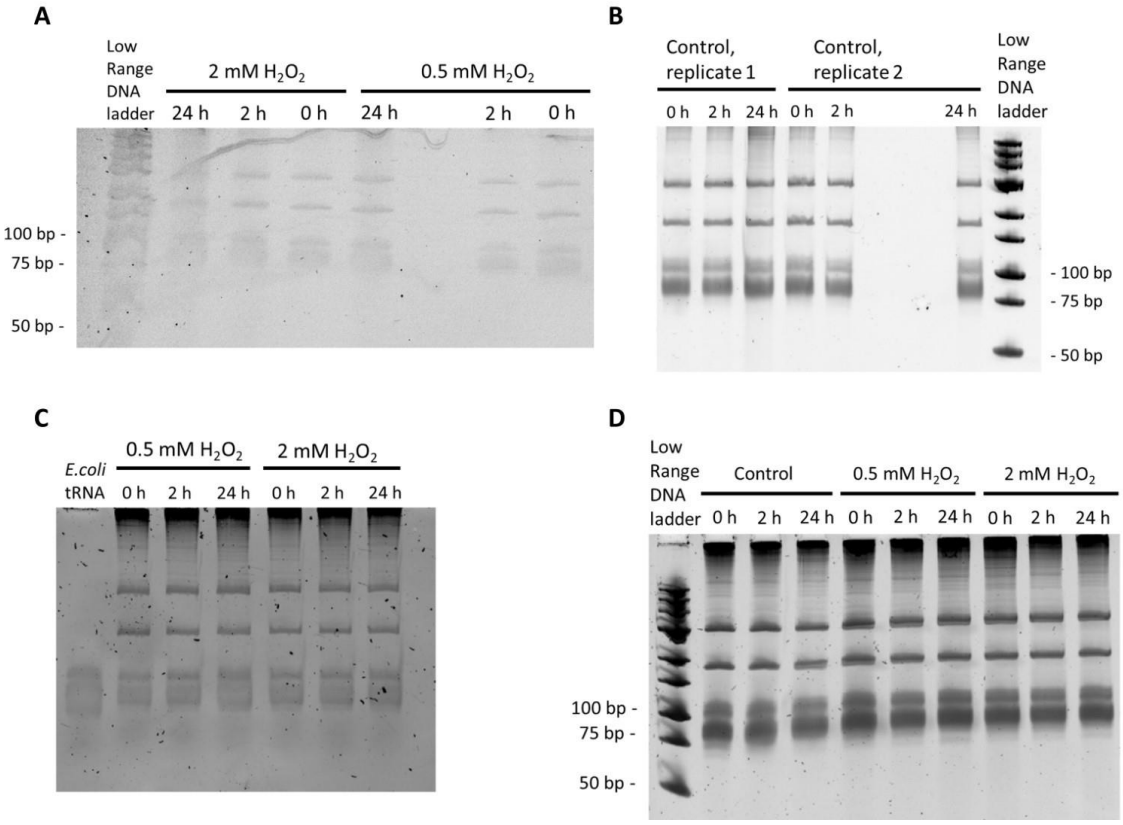

Figure S3. Total RNA quality check on denaturing urea PAA (10%) gel. 500 ng RNA was loaded and stained with SYBR™ Gold. As size reference, Low Range DNA Ladder (Thermo Scientific™) and *E.coli* tRNA (curtsy of Biplu Prajapati, RNAcious Laboratory) were used. Panel A: Replicate 1 total RNA of H_2O_2 treated yeast. Panel B: Replicate 1 and 2 total RNA of control yeast. Panel C: Replicate 2 total RNA of H_2O_2 treated yeast. Panel D: Replicate 3 total RNA of control and H_2O_2 treated yeast.

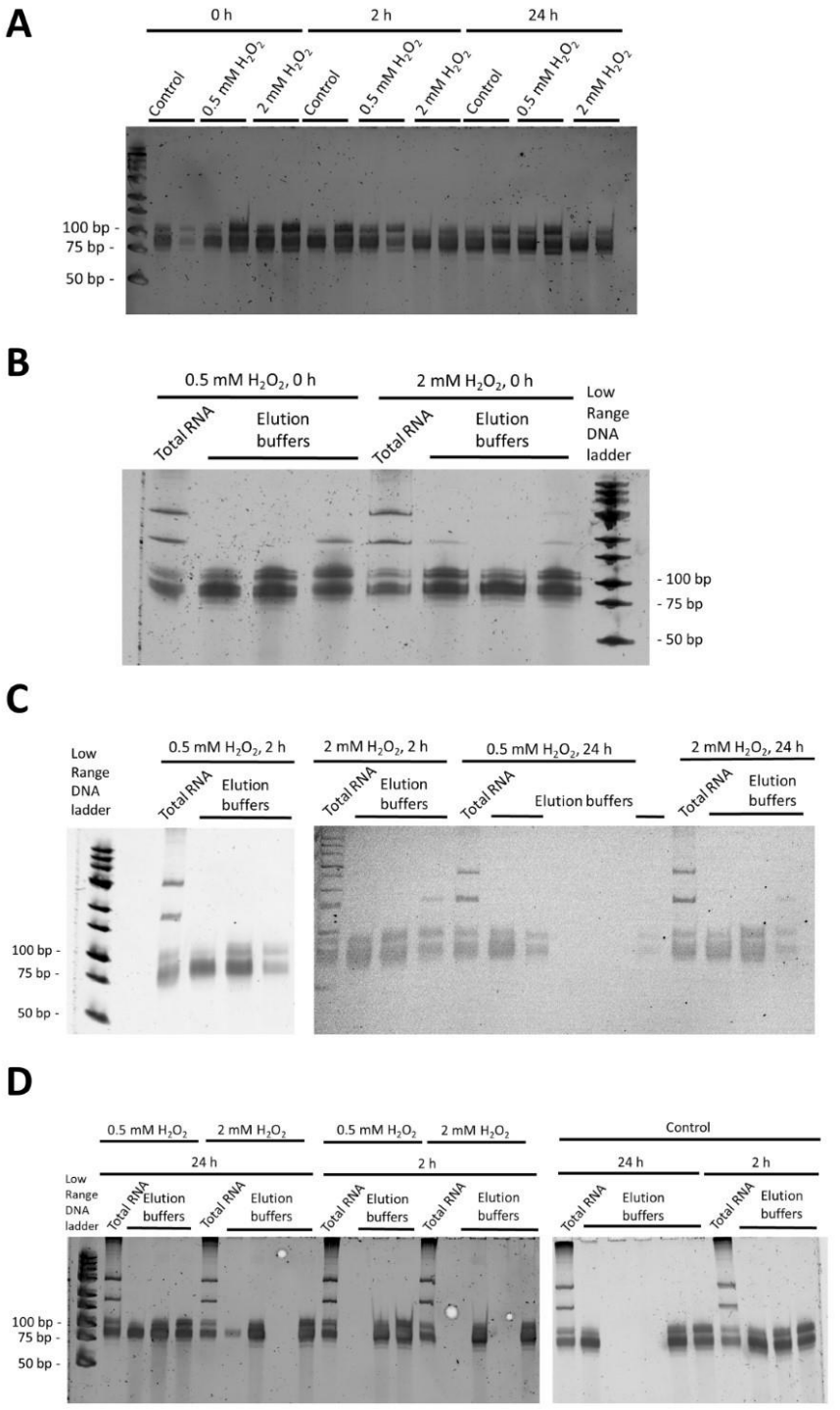

Figure S4. Denaturing polyacrylamide gel (10%) electrophoresis analysis of tRNA isolated from control and H_2O_2 treated yeast. 100 ng RNA was loaded and stained with SYBR™ Gold. As size reference, Low Range DNA Ladder (Thermo Scientific™) was used. Panel A: Biological replicate 1. Each sample is represented with two lanes, as tRNA was isolated with elution buffers containing 750 and 800 mM KCl and checked separately. Panels B and C: Biological replicate 2. Panel D: Biological replicate 3. In B, C and D, each sample is represented with 4 lanes, first one is the total RNA of the respective sample and next 3 lanes are tRNA isolated with 3 elution buffers (containing 700, 750 and 800 mM KCl).

Table S1. Total RNA and transfer RNA isolation yields for control and two treatments, for each of the 3 analyzed timepoints (at hours 0 = elicitation, 2 = stress, 24 = recovery). Data in the table are representing replicate 1.

Treatment	Timepoint (in h)	total RNA yield (µg)	tRNA yield (µg)	tRNA yield (µg) re-isolation
control	0	740	4.779	3.995
control	2	1506	2.361	1.405
control	24	14169	12.897	
0.5 mM	0	775.7	8.210	5.947
0.5 mM	2	1025	7.305	2.908
0.5 mM	24	6636	15.675	
2 mM	0	885.1	6.630	4.787
2 mM	2	653.9	8.235	
2 mM	24	9745.5	13.355	

Table S2. Total RNA and transfer RNA isolation yields for control and two treatments, for each of the 3 analyzed timepoints (at hours 0 = elicitation, 2 = stress, 24 = recovery). Data in the table are representing replicate 2.

Treatment	Timepoint (in h)	total RNA yield (µg)	tRNA yield (µg)
control	0	1303.5	1.85
control	2	4583.5	4.53
control	24	6445	1.825
0.5 mM	0	1157	1.445
0.5 mM	2	2486.5	3.645
0.5 mM	24	5085	5.55
2 mM	0	1632.5	2.02
2 mM	2	1160.5	2.785
2 mM	24	5556.5	4.795

Table S3. Total RNA and transfer RNA isolation yields for control and two treatments, for each of the 3 analyzed timepoints (at hours 0 = elicitation, 2 = stress, 24 = recovery). Data in the table are representing replicate 3.

Treatment	Timepoint (in h)	total RNA yield (µg)	tRNA yield (µg)	tRNA yield (µg) re-isolation
control	0	871.6	1.299	2.510
control	2	3213.2	8.115	
control	24	4003	7.242	
0.5 mM	0	663.5	2.239	2.195
0.5 mM	2	1319.5	3.870	1.5
0.5 mM	24	4462	1.104	1.125
2 mM	0	832.5	4.966	3.105
2 mM	2	4678.5	3.652	4.545
2 mM	24	695	2.180	2.885

8. Acknowledgements

Dr. Peter Sarin for welcoming me into the RNAcious Laboratory, encouraging me to dive into the field of RNA modifications and always pushing forward with new ideas and solutions.

Dr. Ulrike Abendroth for transferring so much of her expert knowledge and excitement for research; every day (and night) support, advice and discussion: Thank you for being the most dedicated supervisor I ever had, despite all the challenges we had working during a pandemic with a tight deadline.

Biplu Prajapati, my fellow master student, lab and office partner, for all the buffers and gels we made together.

Biocomplex core facility, for technical assistance and advice about ultracentrifugation and making all your equipment available for our research.

Dr. Nina Sipari, analytic chemist of Viikki Metabolomics Unit for the UPLC/MS measurements and **Pavlína Gregorová** for organizing the UPLC/MS runs.

Dr. Perttu Seppä, EEB programmer director, and **Dr. Marjo Saastamoinen**, my EEB tutor for help with the smooth start, all administrative matters and studying advice during the master's programmer.

Lena Huovinen, Nicolás Ordax Sommer, Carla Coll Costa, Lluís Serra Domínguez and **Mebin George Varghese** for constantly showing what passion, dedication and hard work look like; for your friendships and all the study and dinner nights spent in Helsinki.

Dorian Jagusch for your friendship since our days spent studying together in Uppsala, all the Ikea trips and science shenanigans we went and will keep going through together.

Nevena Maslać, Marko Kojić and **Stevan Stojanović** for being amazing friends, and the most inspirational and prospective young people I know.

Petnica Science Centre Biology Department where I discovered my passion for biology.

Joni Papponen for being my local in a new land and the most understanding and supporting person in my life.

Milena Stevanović, Sara Milisavljević, Marko Slavuj and **Đorđe Ogrizović** for life-long support and friendship, despite the tremendous physical distances between us currently.

My family for unconditional support in all my scientific and non-scientific endeavors.

9. References

Abegg, M. A., Alabarse, P. V. G., Casanova, A., Hoscheid, J., Salomon, T. B., Hackenhaar, F. S., Medeiros, T. M., & Benfato, M. S. (2010). Response to Oxidative Stress in Eight Pathogenic Yeast Species of the Genus *Candida*. *Mycopathologia*, 170(1), 11–20. https://doi.org/10.1007/s11046-010-9294-5

Acker, M. G., Kolitz, S. E., Mitchell, S. F., Nanda, J. S., & Lorsch, J. R. (2007). Reconstitution of yeast translation initiation. *Methods in Enzymology*, 430, 111–145. https://doi.org/10.1016/S0076-6879(07)30006-2

Alings, F., Sarin, L. P., Fufezan, C., Drexler, H. C. A., & Leidel, S. A. (2015). An evolutionary approach uncovers a diverse response of tRNA 2-thiolation to elevated temperatures in yeast. *RNA* (New York, N.Y.), 21(2), 202–212. https://doi.org/10.1261/rna.048199.114

Behrens, A., Rodschinka, G., & Nedialkova, D. D. (2021). High-resolution quantitative profiling of tRNA abundance and modification status in eukaryotes by mim-tRNAseq. *Molecular Cell*, 81(8), 1802-1815.e7. https://doi.org/https://doi.org/10.1016/j.molcel.2021.01.028

Björk, G. R., Jacobsson, K., Nilsson, K., Johansson, M. J., Byström, A. S., & Persson, O. P. (2001). A primordial tRNA modification required for the evolution of life? *The EMBO Journal*, 20(1–2), 231–239. https://doi.org/10.1093/emboj/20.1.231

Boccaletto, P., Machnicka, M. A., Purta, E., Piątkowski, P., Bagiński, B., Wirecki, T. K., de Crécy-Lagard, V., Ross, R., Limbach, P. A., Kotter, A., Helm, M., & Bujnicki, J. M. (2018). MODOMICS: a database of RNA modification pathways. 2017 update. *Nucleic Acids Research*, 46(D1), D303–D307. https://doi.org/10.1093/nar/gkx1030

Brandmayr, C., Wagner, M., Brückl, T., Globisch, D., Pearson, D., Kneuttinger, A. C., Reiter, V., Hienzsch, A., Koch, S., Thoma, I., Thumbs, P., Michalakis, S., Müller, M., Biel, M., & Carell, T. (2012). Isotope-Based Analysis of Modified tRNA Nucleosides Correlates Modification Density with Translational Efficiency. *Angewandte Chemie International Edition*, 51(44), 11162–11165. https://doi.org/https://doi.org/10.1002/anie.201203769

Briones-Martin-Del-Campo, M., Orta-Zavalza, E., Juarez-Cepeda, J., Gutierrez-Escobedo, G., Cañas-Villamar, I., Castaño, I., & De Las Peñas, A. (2014). The oxidative stress response of the opportunistic fungal pathogen *Candida glabrata*. *Revista Iberoamericana de Micología*, 31(1), 67–71. https://doi.org/https://doi.org/10.1016/j.riam.2013.09.012

Calo, E., Flynn, R. A., Martin, L., Spitale, R. C., Chang, H. Y., & Wysocka, J. (2015). RNA helicase DDX21 coordinates transcription and ribosomal RNA processing. *Nature*, 518(7538), 249–253. https://doi.org/10.1038/nature13923

Chan, C. T. Y., Dyavaiah, M., DeMott, M. S., Taghizadeh, K., Dedon, P. C., & Begley, T. J. (2010). A quantitative systems approach reveals dynamic control of tRNA modifications during cellular stress. *PLoS Genetics*, 6(12), e1001247–e1001247. https://doi.org/10.1371/journal.pgen.1001247

Chen, Y.-T., Hims, M. M., Shetty, R. S., Mull, J., Liu, L., Leyne, M., & Slaugenhaupt, S. A. (2009). Loss of Mouse Ikbkap, a Subunit of Elongator, Leads to Transcriptional Deficits and Embryonic Lethality That Can Be Rescued by Human IKBKAP. *Molecular and Cellular Biology*, 29(3), 736–744. https://doi.org/10.1128/mcb.01313-08

Clark, F. E. (1965). Agar-Plate Method for Total Microbial Count. *Methods of Soil Analysis*. https://doi.org/https://doi.org/10.2134/agronmonogr9.2.c48

Collart, M. A., & Oliviero, S. (1993). Preparation of Yeast RNA. *Current Protocols in Molecular Biology*, 23(1), 13.12.1-13.12.5. https://doi.org/https://doi.org/10.1002/0471142727.mb1312s23

Dauden, M. I., Jaciuk, M., Weis, F., Lin, T.-Y., Kleindienst, C., Abbassi, N. E. H., Khatter, H., Krutyhołowa, R., Breunig, K. D., Kosinski, J., Müller, C. W., & Glatt, S. (2019). Molecular basis of tRNA recognition by the Elongator complex. *Science Advances*, 5(7), eaaw2326. https://doi.org/10.1126/sciadv.aaw2326

Demeshkina, N., Jenner, L., Westhof, E., Yusupov, M., & Yusupova, G. (2012). A new understanding of the decoding principle on the ribosome. *Nature*, 484(7393), 256–259. https://doi.org/10.1038/nature10913

Devi, M., & Lyngdoh, R. H. D. (2018). Favored and less favored codon–anticodon duplexes arising from the GC codon family box encoding for alanine: some computational perspectives. *Journal of Biomolecular Structure and Dynamics*, 36(4), 1029–1049. https://doi.org/10.1080/07391102.2017.1308886

Edelheit, S., Schwartz, S., Mumbach, M. R., Wurtzel, O., & Sorek, R. (2013). Transcriptome-Wide Mapping of 5-methylcytidine RNA Modifications in Bacteria, Archaea, and Yeast Reveals m^5C within Archaeal mRNAs. *PLOS Genetics*, 9(6), e1003602. https://doi.org/10.1371/journal.pgen.1003602

Eichler, D. C., & Craig, N. (1994). Processing of Eukaryotic Ribosomal RNA. In W. E. Cohn & K. B. T.-P. in N. A. R. and M. B. Moldave (Eds.) (Vol. 49, pp. 197–239). Academic Press. https://doi.org/https://doi.org/10.1016/S0079-6603(08)60051-3

Fernández-Vázquez, J., Vargas-Pérez, I., Sansó, M., Buhne, K., Carmona, M., Paulo, E., Hermand, D., Rodriguez-Gabriel, M., Ayté, J., Leidel, S., & Hidalgo, E. (2013). Modification of tRNA(Lys) UUU by elongator is essential for efficient translation of stress mRNAs. *PLoS Genetics*, 9(7), e1003647–e1003647. https://doi.org/10.1371/journal.pgen.1003647

Ferretti, M. B., & Karbstein, K. (2019). Does functional specialization of ribosomes really exist? *RNA* (New York, N.Y.), 25(5), 521–538. https://doi.org/10.1261/rna.069823.118

Gilbert, W. V. (2011). Functional specialization of ribosomes? *Trends in Biochemical Sciences*, 36(3), 127–132. https://doi.org/https://doi.org/10.1016/j.tibs.2010.12.002

Globisch, D., Pearson, D., Hienzsch, A., Brückl, T., Wagner, M., Thoma, I., Thumbs, P., Reiter, V., Kneuttinger, A. C., Müller, M., Sieber, S. A., & Carell, T. (2011). Systems-based analysis of modified tRNA bases. *Angewandte Chemie - International Edition*, 50(41), 9739–9742. https://doi.org/10.1002/anie.201103229

Gokhale, N. S., & Horner, S. M. (2017). RNA modifications go viral. *PLOS Pathogens*, 13(3), e1006188. https://doi.org/10.1371/journal.ppat.1006188

Granneman, S., Petfalski, E., & Tollervey, D. (2011). A cluster of ribosome synthesis factors regulate pre-rRNA folding and 5.8S rRNA maturation by the Rat1 exonuclease. *The EMBO Journal*, 30(19), 4006–4019. https://doi.org/https://doi.org/10.1038/emboj.2011.256

Gregorova, P., Sipari, N. H., & Sarin, L. P. (2020). Broad-range RNA modification analysis of complex biological samples using rapid C18-UPLC-MS. *RNA Biology*, 1–8. https://doi.org/10.1080/15476286.2020.1853385

Grosjean, H., Breton, M., Sirand-Pugnet, P., Tardy, F., Thiaucourt, F., Citti, C., Barre, A., Yoshizawa, S., Fourmy, D., de Crecy-Lagard, V., & Blanchard, A. (2014). Predicting the minimal translation apparatus: lessons from the reductive evolution of mollicutes. *PLoS Genetics*, 10(5), e1004363–e1004363. https://doi.org/10.1371/journal.pgen.1004363

Haeusler, R. A., Pratt-Hyatt, M., Good, P. D., Gipson, T. A., & Engelke, D. R. (2008). Clustering of yeast tRNA genes is mediated by specific association of condensin with tRNA gene transcription complexes. *Genes & Development*, 22(16), 2204–2214. https://doi.org/10.1101/gad.1675908

Heiss, M., Reichle, V. F., & Kellner, S. (2017). Observing the fate of tRNA and its modifications by nucleic acid isotope labeling mass spectrometry: NAIL-MS. *RNA Biology*, 14(9), 1260–1268. https://doi.org/10.1080/15476286.2017.1325063

Helm, M. (2006). Post-transcriptional nucleotide modification and alternative folding of RNA. *Nucleic Acids Research*, 34(2), 721–733. https://doi.org/10.1093/nar/gkj471

Hibi, K., Amikura, K., Sugiura, N., Masuda, K., Ohno, S., Yokogawa, T., Ueda, T., & Shimizu, Y. (2020). Reconstituted cell-free protein synthesis using in vitro transcribed tRNAs. *Communications Biology*, 3(1), 350. https://doi.org/10.1038/s42003-020-1074-2

Holcik, M., & Sonenberg, N. (2005). Translational control in stress and apoptosis. *Nature Reviews Molecular Cell Biology*, 6(4), 318–327. https://doi.org/10.1038/nrm1618

Hopper, A. K., & Phizicky, E. M. (2003). tRNA transfers to the limelight. *Genes and Development*, 17(2), 162–180. https://doi.org/10.1101/gad.1049103

Huh, D., Passarelli, M. C., Gao, J., Dusmatova, S. N., Goin, C., Fish, L., Pinzaru, A. M., Molina, H., Ren, Z., McMillan, E. A., Asgharian, H., Goodarzi, H., & Tavazoie, S. F. (2021). A stress-induced tyrosine-tRNA depletion response mediates codon-based translational repression and growth suppression. *The EMBO Journal*, 40(2), e106696. https://doi.org/https://doi.org/10.15252/embj.2020106696

Ishiguro, J. (1976). Study on proteins from yeast cytoplasmic ribosomes by two-dimensional gel electrophoresis. *Molecular and General Genetics*, 145(1), 73–79. https://doi.org/10.1007/BF00331560

Iwata-Reuyl, D. (2008). An embarrassment of riches: the enzymology of RNA modification. *Current Opinion in Chemical Biology*, 12(2), 126–133. https://doi.org/10.1016/j.cbpa.2008.01.041

Johansson, M. J. O., Esberg, A., Huang, B., Björk, G. R., & Byström, A. S. (2008). Eukaryotic wobble uridine modifications promote a functionally redundant decoding system. *Molecular and Cellular Biology*, 28(10), 3301–3312. https://doi.org/10.1128/MCB.01542-07

Jora, M., Borland, K., Abernathy, S., Zhao, R., Kelley, M., Kellner, S., Addepalli, B., & Limbach, P. A. (2021). Chemical Amination/Imination of Carbonothiolated Nucleosides During RNA Hydrolysis. *Angewandte Chemie International Edition*, 60(8), 3961–3966. https://doi.org/https://doi.org/10.1002/anie.202010793

Katajamaa, M., Miettinen, J., & Orešič, M. (2006). MZmine: toolbox for processing and visualization of mass spectrometry based molecular profile data. *Bioinformatics*, 22(5), 634–636. https://doi.org/10.1093/bioinformatics/btk039

Khan, M. S. N., Salim, M., & Maden, B. E. H. (1978). Extensive homologies between the methylated nucleotide sequences in several vertebrate ribosomal ribonucleic acids. *Biochemical Journal*, 169(3), 531–542. https://doi.org/10.1042/bj1690531

Kierzek, E., & Kierzek, R. (2003). The thermodynamic stability of RNA duplexes and hairpins containing N6-alkyladenosines and 2-methylthio-N6-alkyladenosines. *Nucleic Acids Research*, 31(15), 4472–4480. https://doi.org/10.1093/nar/gkg633

Kim, Y.-K., Heo, I., & Kim, V. N. (2010). Modifications of small RNAs and their associated proteins. *Cell*, 143(5), 703–709. https://doi.org/10.1016/j.cell.2010.11.018

Klootwijk, J., & Planta, R. J. (1973). Analysis of the Methylation Sites in Yeast Ribosomal RNA. European *Journal of Biochemistry*, 39(2), 325–333. https://doi.org/https://doi.org/10.1111/j.1432-1033.1973.tb03130.x

Kobayashi, T., Heck, D. J., Nomura, M., & Horiuchi, T. (1998). Expansion and contraction of ribosomal DNA repeats in *Saccharomyces cerevisiae*: requirement of replication fork blocking (Fob1) protein and the role of RNA polymerase I. *Genes & Development*, 12(24), 3821–3830. https://doi.org/10.1101/gad.12.24.3821

Koh, C. S., & Sarin, L. P. (2018). Transfer RNA modification and infection – Implications for pathogenicity and host responses. *Biochimica et Biophysica Acta - Gene Regulatory Mechanisms*, 1861(4), 419–432. https://doi.org/10.1016/j.bbagrm.2018.01.015

Lafontaine, D. L. J. (2015). Noncoding RNAs in eukaryotic ribosome biogenesis and function. *Nature Structural & Molecular Biology*, 22(1), 11–19. https://doi.org/10.1038/nsmb.2939

Laxman, S., Sutter, B. M., Wu, X., Kumar, S., Guo, X., Trudgian, D. C., Mirzaei, H., & Tu, B. P. (2013). Sulfur amino acids regulate translational capacity and metabolic homeostasis through modulation of tRNA thiolation. *Cell*, 154(2), 416–429. https://doi.org/10.1016/j.cell.2013.06.043

Leidel, S., Pedrioli, P. G. A., Bucher, T., Brost, R., Costanzo, M., Schmidt, A., Aebersold, R., Boone, C., Hofmann, K., & Peter, M. (2009). Ubiquitin-related modifier Urm1 acts as a sulphur carrier in thiolation of eukaryotic transfer RNA. *Nature*, 458(7235), 228–232. https://doi.org/10.1038/nature07643

Leiva, L. E., Pincheira, A., Elgamal, S., Kienast, S. D., Bravo, V., Leufken, J., Gutierrez, D., Leidel, S. A., Ibba, M., & Katz, A. (2020). Modulation of Escherichia coli Translation by the Specific Inactivation of tRNAGly Under Oxidative Stress. *Frontiers in Genetics*, 11, 856. https://doi.org/10.3389/fgene.2020.00856

Li, X., Xiong, X., & Yi, C. (2017). Epitranscriptome sequencing technologies: decoding RNA modifications. *Nature Methods*, 14(1), 23–31. https://doi.org/10.1038/nmeth.4110

Liu, F., Clark, W., Luo, G., Wang, X., Fu, Y., Wei, J., Wang, X., Hao, Z., Dai, Q., Zheng, G., Ma, H., Han, D., Evans, M., Klungland, A., Pan, T., & He, C. (2016). ALKBH1-Mediated tRNA Demethylation Regulates Translation. *Cell*, 167(3), 816-828.e16. https://doi.org/https://doi.org/10.1016/j.cell.2016.09.038

Machnicka, M. A., Milanowska, K., Oglou, O. O., Purta, E., Kurkowska, M., Olchowik, A., Januszewski, W., Kalinowski, S., Dunin-Horkawicz, S., Rother, K. M., Helm, M., Bujnicki, J. M., & Grosjean, H. (2013). MODOMICS: A database of RNA modification pathways - 2013 update. *Nucleic Acids Research*, 41(D1), 262–267. https://doi.org/10.1093/nar/gks1007

Macon, J. B., & Wolfenden, R. (1968). 1-Methyladenosine. Dimroth rearrangement and reversible reduction. *Biochemistry*, 7(10), 3453–3458. https://doi.org/10.1021/bi00850a021

Maden, B. E. H. (1988). Locations of methyl groups in 28 S rRNA of *Xenopus laevis* and man: Clustering in the conserved core of molecule. *Journal of Molecular Biology*, 201(2), 289–314. https://doi.org/https://doi.org/10.1016/0022-2836(88)90139-8

Maden, B. E. H., & Salim, M. (1974). The methylated nucleotide sequences in HeLa cell ribosomal RNA and its precursors. *Journal of Molecular Biology*, 88(1), 133–152. https://doi.org/https://doi.org/10.1016/0022-2836(74)90299-X

McMahon, M., Contreras, A., & Ruggero, D. (2015). Small RNAs with big implications: new insights into H/ACA snoRNA function and their role in human disease. *WIREs RNA*, 6(2), 173–189. https://doi.org/https://doi.org/10.1002/wrna.1266

Myers, O. D., Sumner, S. J., Li, S., Barnes, S., & Du, X. (2017). One Step Forward for Reducing False Positive and False Negative Compound Identifications from Mass Spectrometry Metabolomics Data: New Algorithms for Constructing Extracted Ion Chromatograms and Detecting Chromatographic Peaks. *Analytical Chemistry*, 89(17), 8696–8703. https://doi.org/10.1021/acs.analchem.7b00947

Näsvall, S. J., Chen, P., & Björk, G. R. (2007). The wobble hypothesis revisited: uridine-5-oxyacetic acid is critical for reading of G-ending codons. *RNA* (New York, N.Y.), 13(12), 2151–2164. https://doi.org/10.1261/rna.731007

Nawrot, B., Sochacka, E., & Düchler, M. (2011). tRNA structural and functional changes induced by oxidative stress. *Cellular and Molecular Life Sciences*, 68(24), 4023–4032. https://doi.org/10.1007/s00018-011-0773-8

Nedialkova, D. D., & Leidel, S. A. (2015). Optimization of Codon Translation Rates via tRNA Modifications Maintains Proteome Integrity. *Cell*, 161(7), 1606–1618. https://doi.org/https://doi.org/10.1016/j.cell.2015.05.022

Nicoll, W. D., & Smith, A. F. (1955). Stability of Dilute Alkaline Solutions of Hydrogen Peroxide. Industrial & *Engineering Chemistry*, 47(12), 2548–2554. https://doi.org/10.1021/ie50552a051

Noma, A., Sakaguchi, Y., & Suzuki, T. (2009). Mechanistic characterization of the sulfur-relay system for eukaryotic 2-thiouridine biogenesis at tRNA wobble positions. *Nucleic Acids Research*, 37(4), 1335–1352. https://doi.org/10.1093/nar/gkn1023

Nyström, T. (2004). Stationary-Phase Physiology. *Annual Review of Microbiology*, 58(1), 161–181. https://doi.org/10.1146/annurev.micro.58.030603.123818

Pabis, M., Termathe, M., Ravichandran, K. E., Kienast, S. D., Krutyhołowa, R., Sokołowski, M., Jankowska, U., Grudnik, P., Leidel, S. A., & Glatt, S. (2020). Molecular basis for the bifunctional Uba4–Urm1 sulfur-relay system in tRNA thiolation and ubiquitin-like conjugation. *The EMBO Journal*, 39(19), e105087. https://doi.org/https://doi.org/10.15252/embj.2020105087

Penzo, M., & Montanaro, L. (2018). Turning Uridines around: Role of rRNA Pseudouridylation in Ribosome Biogenesis and Ribosomal Function. *Biomolecules*. https://doi.org/10.3390/biom8020038

Perche-Letuvée, P., Molle, T., Forouhar, F., Mulliez, E., & Atta, M. (2014). Wybutosine biosynthesis: Structural and mechanistic overview. *RNA Biology*, 11(12), 1508–1518. https://doi.org/10.4161/15476286.2014.992271

Piñeyro, D., Torres, A. G., & de Pouplana, L. R. (2014). Biogenesis and Evolution of Functional tRNAs BT - Fungal RNA Biology. In A. Sesma & T. von der Haar (Eds.) (pp. 233–267). Cham: Springer International Publishing. https://doi.org/10.1007/978-3-319-05687-6_10

Planta, R. J., & Mager, W. H. (1998). The list of cytoplasmic ribosomal proteins of *Saccharomyces cerevisiae*. *Yeast*, 14(5), 471–477. https://doi.org/https://doi.org/10.1002/(SICI)1097-0061(19980330)14:5<471::AID-YEA241>3.0.CO;2-U

Pluskal, T., Castillo, S., Villar-Briones, A., & Orešič, M. (2010). MZmine 2: Modular framework for processing, visualizing, and analyzing mass spectrometry-based molecular profile data. *BMC Bioinformatics*, 11(1), 395. https://doi.org/10.1186/1471-2105-11-395

Puri, P., Wetzel, C., Saffert, P., Gaston, K. W., Russell, S. P., Cordero Varela, J. A., van der Vlies, P., Zhang, G., Limbach, P. A., Igntova, Z., & Poolman, B. (2014). Systematic identification of tRNAome and its dynamics in *Lactococcus lactis*. *Molecular Microbiology*, 93(5), 944–956. https://doi.org/https://doi.org/10.1111/mmi.12710

Rezgui, V. A. N., Tyagi, K., Ranjan, N., Konevega, A. L., Mittelstaet, J., Rodnina, M. V, Peter, M., & Pedrioli, P. G. A. (2013). tRNA tKUUU, tQUUG, and tEUUC wobble position modifications fine-tune protein translation by promoting ribosome A-site binding. *Proceedings of the National Academy of Sciences of the United States of America*, 110(30), 12289–12294. https://doi.org/10.1073/pnas.1300781110

Rodger, A. (2013). UV Absorbance Spectroscopy of Biological Macromolecules BT - Encyclopedia of Biophysics. In G. C. K. Roberts (Ed.) (pp. 2714–2718). Berlin, Heidelberg: Springer Berlin Heidelberg. https://doi.org/10.1007/978-3-642-16712-6_780

Rozov, A., Demeshkina, N., Khusainov, I., Westhof, E., Yusupov, M., & Yusupova, G. (2016). Novel base-pairing interactions at the tRNA wobble position crucial for accurate reading of the genetic code. *Nature Communications*, 7(1), 10457. https://doi.org/10.1038/ncomms10457

Sakai, K., Ohta, T., Minoshima, S., Kudoh, J., Wang, Y., de Jong, P. J., & Shimizu, N. (1995). Human ribosomal RNA gene cluster: identification of the proximal end containing a novel tandem repeat sequence. Genomics, 26(3), 521–526. https://doi.org/10.1016/0888-7543(95)80170-q

Sarin, L. P., Kienast, S. D., Leufken, J., Ross, R. L., Dziergowska, A., Debiec, K., Sochacka, E., Limbach, P. A., Fufezan, C., Drexler, H. C. A., & Leidel, S. A. (2018). Nano LC-MS using capillary columns enables accurate quantification of modified ribonucleosides at low femtomol levels. *RNA* (New York, N.Y.), 24(10), 1403–1417. https://doi.org/10.1261/rna.065482.117

Sarin, L. P., & Leidel, S. A. (2014). Modify or die? - RNA modification defects in metazoans. *RNA Biology*, 11(12), 1555–1567. https://doi.org/10.4161/15476286.2014.992279

Schaffrath, R., & Leidel, S. A. (2017). Wobble uridine modifications-a reason to live, a reason to die?! *RNA Biology*, 14(9), 1209–1222. https://doi.org/10.1080/15476286.2017.1295204

Sharma, S., & Lafontaine, D. L. J. (2015). 'View From A Bridge': A New Perspective on Eukaryotic rRNA Base Modification. *Trends in Biochemical Sciences*, 40(10), 560–575. https://doi.org/https://doi.org/10.1016/j.tibs.2015.07.008

Shi, J., Zhang, Y., Tan, D., Zhang, X., Yan, M., Zhang, Y., Fraklin, R., Shahbazi, M., Mackinlay, K., Liu, S., Kuhle, B., James, E. R., Zhang, L., Qu, Y., Zhai, Q., Zhao, W., Zhao, L., Zhou, C., Gu, W., Murn, J., Guo, J., Carrell, D. T., Wang, Y., Chen, X., Cairns, B. R., Yang, X., Schimmel, P., Zernicka-Goetz, M., Cheloufi, S., Zhang, Y., Zhou, T., & Chen, Q. (2021). PANDORA-seq expands the repertoire of regulatory small RNAs by overcoming RNA modifications. *Nature Cell Biology*, 23(4), 424–436. https://doi.org/10.1038/s41556-021-00652-7

Shigematsu, M., Honda, S., Loher, P., Telonis, A. G., Rigoutsos, I., & Kirino, Y. (2017). YAMAT-seq: an efficient method for high-throughput sequencing of mature transfer RNAs. *Nucleic Acids Research*, 45(9), e70–e70. https://doi.org/10.1093/nar/gkx005

Sloan, K. E., Warda, A. S., Sharma, S., Entian, K.-D., Lafontaine, D. L. J., & Bohnsack, M. T. (2017). Tuning the ribosome: The influence of rRNA modification on eukaryotic ribosome biogenesis and function. *RNA Biology*, 14(9), 1138–1152. https://doi.org/10.1080/15476286.2016.1259781

Song, H., Liu, D., Dong, S., Zeng, L., Wu, Z., Zhao, P., Zhang, L., Chen, Z., & Zou, C. (2020). Epitranscriptomics and epiproteomics in cancer drug resistance: therapeutic implications. *Signal Transduction and Targeted Therapy*, 5(1), 193. https://doi.org/10.1038/s41392-020-00300-w

Squires, J. E., Patel, H. R., Nousch, M., Sibbritt, T., Humphreys, D. T., Parker, B. J., Suter, C. M., & Preiss, T. (2012). Widespread occurrence of 5-methylcytosine in human coding and non-coding RNA. *Nucleic Acids Research*, 40(11), 5023–5033. https://doi.org/10.1093/nar/gks144

Sun, C., Jora, M., Solivio, B., Limbach, P. A., & Addepalli, B. (2018). The Effects of Ultraviolet Radiation on Nucleoside Modifications in RNA. *ACS Chemical Biology*, 13(3), 567–572. https://doi.org/10.1021/acschembio.7b00898

Thompson, D. M., Lu, C., Green, P. J., & Parker, R. (2008). tRNA cleavage is a conserved response to oxidative stress in eukaryotes. *RNA* (New York, N.Y.), 14(10), 2095–2103. https://doi.org/10.1261/rna.1232808

Thompson, D. M., & Parker, R. (2009). Stressing Out over tRNA Cleavage. *Cell*, 138(2), 215–219. https://doi.org/10.1016/j.cell.2009.07.001

Turner, J. J., Ewald, J. C., & Skotheim, J. M. (2012). Cell size control in yeast. *Current Biology*, 22(9), R350–R359. https://doi.org/10.1016/j.cub.2012.02.041

Vandivier, L. E., Anderson, Z. D., & Gregory, B. D. (2019). HAMR: High-Throughput Annotation of Modified Ribonucleotides. In N. Wajapeyee & R. Gupta (Eds.), Epitranscriptomics: Methods and Protocols (pp. 51–67). New York, NY: Springer New York. https://doi.org/10.1007/978-1-4939-8808-2_4

Wang, X., Matuszek, Z., Huang, Y., Parisien, M., Dai, Q., Clark, W., Schwartz, M. H., & Pan, T. (2018). Queuosine modification protects cognate tRNAs against ribonuclease cleavage. *RNA*, 24(10), 1305–1313. https://doi.org/10.1261/rna.067033.118

Watson, J. D. (2014). Molecular biology of the gene (Seventh edition.). Boston: Pearson.

Woolford Jr, J. L., & Baserga, S. J. (2013). Ribosome biogenesis in the yeast *Saccharomyces cerevisiae*. *Genetics*, 195(3), 643–681. https://doi.org/10.1534/genetics.113.153197

Yang, J., Sharma, S., Watzinger, P., Hartmann, J. D., Kötter, P., & Entian, K.-D. (2016). Mapping of Complete Set of Ribose and Base Modifications of Yeast rRNA by RP-HPLC and Mung Bean Nuclease Assay. *PLOS ONE*, 11(12), e0168873. https://doi.org/10.1371/journal.pone.0168873

Zhang, N., Shi, S., Yoo, B., Yuan, X., Li, W., & Zhang, S. (2020). 2D-HELS MS Seq: A General LC-MS-Based Method for Direct and de novo Sequencing of RNA Mixtures with Different Nucleotide Modifications. *JoVE*, (161), e61281. https://doi.org/doi:10.3791/61281

Zhang, X., Walker, R. C., Phizicky, E. M., & Mathews, D. H. (2014). Influence of Sequence and Covalent Modifications on Yeast tRNA Dynamics. *Journal of Chemical Theory and Computation*, 10(8), 3473–3483. https://doi.org/10.1021/ct500107y

Zinshteyn, B., & Gilbert, W. V. (2013). Loss of a Conserved tRNA Anticodon Modification Perturbs Cellular Signaling. *PLOS Genetics*, 9(8), e1003675. https://doi.org/10.1371/journal.pgen.1003675